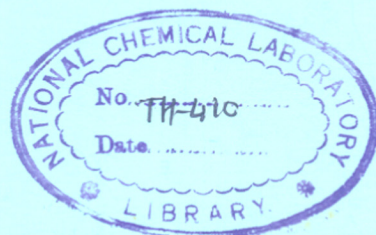# PHYSICO-CHEMICAL CHARACTERISATION OF ZSM–5 TYPE ZEOLITES

A THESIS
SUBMITTED TO THE
UNIVERSITY OF POONA
IN PARTIAL FULFILMENT
FOR THE DEGREE OF
MASTER OF SCIENCE
(IN CHEMISTRY)

BY
VILAS RAMDAS CHUMBHALE
B. Sc. (Hons.)

PHYSICAL CHEMISTRY DIVISION
NATIONAL CHEMICAL LABORATORY
PUNE - 411008 (INDIA)
1984

Dedicated to my parents
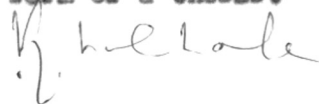
COMPUTERISED

A C K N O W L E D G E M E N T

It gives me immense pleasure to record my
deep sense of gratitude to Dr.(Miss) S. B. Kulkarni,
for her meticulous planning and inspiring guidance
through out this investigation and also for the pains-
taking efforts in the preparation of the manuscript.

I am grateful to Dr. P. Ratnasamy for his
valuable advice and helpful suggestions during the study.

I wish to sincerely acknowledge the kind coope-
ration and help rendered by my colleagues and friends,
at all the stages of this work.

Finally, I am grateful to the Director,
National Chemical Laboratory, Poona-8, for allowing me
to submit this investigation in the form of a thesis.

(V. R. CHUMBHALE)

POONA,
10th May 1984.

C O N T E N T S

---OOO---

CHAPTER-1

INTRODUCTION

1.1. INTRODUCTION

Zeolites are crystalline aluminosilicates represented by the formula : $M_{2/n}O$, Al_2O_3, $XSiO_2$, YH_2O where M is a cation of valence n. The zeolite structure consists of a three dimensional net-work of AlO_4 and SiO_4 tetrahedra linked to each other by sharing the oxygen ions. The excess negative charge on the aluminum ion is balanced by an alkali metal ion which can be partially or completely exchanged with other mono-, di- or trivalent ions. The SiO_4, AlO_4 net-work forms honey-combed structure consisting of cavities and channels of molecular dimensions.

The nature of cations profoundly affects the pore size in the zeolite which in turn changes the sorption and catalytic properties of the zeolites. As a result of their unique structural properties, zeolites have been employed extensively in petrochemical and allied industries as adsorbents for separation of hydrocarbon and as shape selective catalysts for cracking, isomerization, selecto-forming and transformation of aromatic hydrocarbons.

1.2. HISTORICAL BACKGROUND

The history of zeolites began with the discovery of stilbite in 1756 by the Swedish mineralogist, Cronsted[1]. The name zeolite signifies "boiling stone". Zeolite minerals have been recognised as widespread components in

basaltic rocks and are found in many parts of the world.
A reversible dehydration[2] of the zeolite crystals and
adsorption[3] of gases in dehydrated chabazite were observed
in early 19th century. Barrer[4,5] and coworkers carried out
systematic investigations on the synthesis, structure and
adsorption properties of a large number of zeolites.
Simultaneously, at the Union Carbide, Linde Division, Milton[6]
and his associates carried out commercial development of
molecular sieve zeolites designated as A, X and Y. However,
a major break through in zeolite technology came in 1962 when
Mobil Oil Co. (U.S.A.) introduced the zeolites for catalytic
cracking reactions in petroleum processing. Since then, zeolite
catalysis has undergone rapid and dynamic advances, as is
evident from the tremendous scientific and technical literature
exceeding 25000 articles and more than 5000 (U.S.) patents. The
crystal structure of forty zeolite minerals has been established
to date and over 150 synthetic zeolites have been reported[7] in
literature.

The major industrial processes that use zeolite
catalysts are listed in Table 1.1, together with their respective
zeolite usages. Three of the milestones that formed the founda-
tion for the discoveries and break throughs in industrial
processes are[7] (1) the introduction of commercial catalytic
cracking in (1964), (2) the demonstration of shape selectivity
in chemical reactions (1962), and (3) use of organic cations
as templates for zeolite synthesis.

TABLE - 1.1

APPLICATIONS OF ZEOLITES *

Process	Probable zeolite catalyst	Competitive features
Catalytic cracking	X and Y	Improved yields. Reduced light gas and coke.
Isomerization	Y, Mordenite	High selectivity and resistance to high poisoning
Catalytic reforming	Y, Mordenite	Activators, unnecessary high selectivity.
Polymerization	Y	Non-corrosive.
Alkylation	Y, HZSM5	Non-corrosive, feed treatment minimized.
Hydrode-alkylation	X and Y	High activity and improved selectivity.
Hydrogenation	X and Y	Resistance to S poisoning.
Selective hydrogenation	A	Separation problems minimized.
Methanation	X and Y	High yields, resistance to poisons.
Dehydrogenation	X and Y	Improved selectivity.
Dehydration	A	Improved rates and yields.
Dehydrohalogenation	A	Molecular size selectivity.

* Ref: P.E. Pickert, A.P. Botton and M.A. Lanewala
Chem.Engn., 75(16), 133 (1968).

Using tetramethyl ammonium ion, Barrer[8] synthesized (N-A), (N-X) and (N-Y) zeolites. Kerr[9] observed that organic cations facilitate the synthesis of new zeolites. He first synthesized zeolites ZK-4 and ZK-5. These break throughs were followed rapidly by the synthesis of many zeolites from organic cation containing mixtures such as omega[10], ZSM-4[11] and ZSM-5[12]. The most important amongst these is Zeolite Socony Mobil designated ZSM5.

Since Mobil Oil Corporation introduced a new shape selective high silica ZSM5 zeolite, a number of commercially important catalysts and processes have been developed, which are listed in Table 1.2.

The ZSM5 type zeolites possess the following unique properties:

1.   High thermal stability (> 1283 K) and stability to most mineral acids. They also show structural stability[13] to steam under catalytic reaction conditions.

2.   Molecular shape selectivity[14] arising from the unique pore dimensions (5.6-6$\overset{o}{A}$) offering both steric restrictions at the active sites and occurance of preferential diffusion paths[15].

3.   The constraint that, normally, hydrocarbons containing more than 10 carbon atoms are not formed in the methanol to gasoline conversion[16] on ZSM5 zeolites, which is also true of other processes.

The unique catalytic properties of zeolite including its high resistance towards deactivation due to coking are

TABLE - 1.2

INDUSTRIAL PROCESSES BASED ON SHAPE
SELECTIVE ZEOLITES*

Process	Objective	Major chemical process characterisation
Selectoforming	Octane number is increased in gasoline LPG production.	Selective n-paraffin cracking.
M-forming	High yield, octane number increases in gasoline.	Cracking depending on degree of branching aromatic alkylation and cracking fragments.
Dewaxing	Light fuel from heavy fuel oil. Lube oil with low temperature pour point.	Cracking of high molecular weight, n- and monomethyl paraffins.
Xylene isomerization	High yield of p-xylene product.	High through put long cycle life, suppression of side reactions.
Ethylbenzene	High yield of ethylbenzene, elimination of $AlCl_3$ handling	
Toluene disproportionation	Benzene and xylenes from toluene.	
Methanol to gasoline.	Methanol (from coal or natural gas), conversion to high grade gasoline.	Synthesis of hydrocarbons only, restricted to gasoline range (C_4 to C_{10}) including aromatics.

* Ref: Weisz, P.B., Pure and Applied Chem., 52, 2091 (1980).

attributed[17,18] to the presence of strong acid sites as well as unique molecular shape selective properties imparted to the zeolites by the three dimensional system of intersecting channels.

The structural adsorption and catalytic properties of ZSM5 type zeolites are reviewed in the following sections.

1.3.   CHARACTERISTICS OF ZSM5 ZEOLITES

(A) Structure of ZSM5

The ZSM5 belongs to a pentasil family of zeolites and has a unique channel structure which differs from the large pore X and Y zeolites and small pore zeolites such as Linde A and erionite. As reported by Kokotailo et al[17], the framework of ZSM5 zeolite is composed of a novel configuration of linked tetrahedra which are bound together in groups consisting of eight five-membered rings as shown in Fig. 1a. These building units are attached to each other through edges to form chains as shown in Fig. 1b. The chains are then connected to form planes, and the linking of the planes gives three dimensional framework structure. The planes parallel to (100) and (010) are illustrated in Figs. 1c and 1d respectively.

The as synthesized, uncalcined ZSM5 zeolite generally exhibits orthorhombic symmetry with lattice parameters a = 20.1 $\overset{\circ}{A}$, b = 19.9 $\overset{\circ}{A}$ and c = 13.4 $\overset{\circ}{A}$. However, reversible transformation to monoclinic symmetry has been reported[18] due to calcination and ion exchange. The composition of the unit cell in the Na form
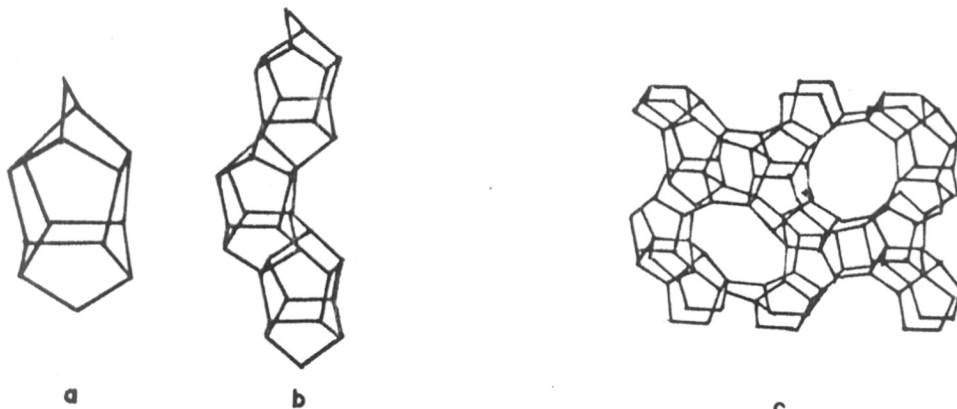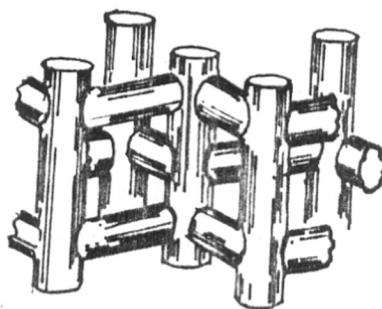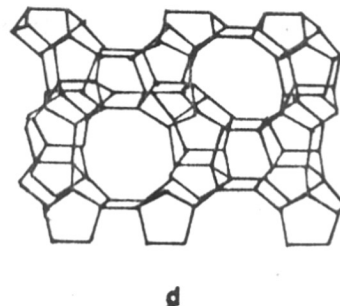
a) CHARACTERISTIC CONFIGURATION
   OF ZSM-5
b) LINKAGE OF ZSM-5

c) SKELETAL DIAGRAM OF O1O FACE

d) SKELETAL DIAGRAM OF 100 FACE

e) CHANNEL STRUCTURE OF
   ZSM-5 ZEOLITE

FIG. 1. STRUCTURE OF ZSM-5 ZEOLITE.

is $Na_nAl_nSi_{96-n}O_{192}.16H_2O$ where n < 27 and typically[12] about

3. The number of Al atoms per unit cell is calculated as

$$Na_{Al} = \frac{96}{1 + R}$$

where $R = \frac{N_{Si}}{N_{Al}}$, N_{Si} and N_{Al} being the gram atoms of Si and Al respectively.

The ZSM5 framework consists of two intersecting channel systems, one sinusoidal running parallel to 001 and the other straight and parallel to (010) as shown in Fig. 1e. The sinusoidal channel has near circular opening (5.4-5.6$\overset{o}{A}$) and the straight channel has elliptical opening (5.2-5.8$\overset{o}{A}$). A similar framework structure has been found[19] in silicalite which is Al free three dimensional crystalline SiO_2.

(B) Sorption and Diffusion in ZSM5 zeolites

In molecular shape selective catalysis, the effective pore opening and channel dimension play important roles in controlling the type of material that react and the products formed. The sorption and diffusion data are helpful in understanding the product distribution in catalytic reaction. In ZSM5 the n-paraffins and monomethyl paraffins diffuse more rapidly than monocyclic hydrocarbons which in turn diffuse more rapidly than dimethyl substituted paraffins. Anderson et al[20] have compaired the adsorption behaviour of some hydrocarbons on NaZSM5 and HZSM5 zeolites and have classified the sorbents into two categories:

(1)   Fast adsorption which includes n hexane, toluene and p-xylene,

(2)   Slow sorption which occurs with 2,3 dimethyl butane, o-xylene and 1,3,5 trimethyl benzene. The lower accessibility of the inner pore structure of ZSM5 was attributed to this behaviour.

Similar studies have been reported on silicalite[19] and ZSM5 of different Si/Al ratios[21] and it is observed that the ion exchange capacity, the catalytic activity and hydrophobicity are linearly dependent on the Al content.

(C) Ion Exchange

The ion exchange characteristics of ZSM5 have been examined by Chu et al[22] for a wide spectrum of cations using a variety of morphological and compositional forms of zeolite. It was found that the ion selectivities in ZSM5 were considerably different from those of the conventional synthetic zeolites A, X and Y. The overall selectivity ranking of the alkali metals and NH_4^+ and divalent ions is found to be:

$$Cs^+ > NH_4^+ > K^+ > Na^+ > Li^+, \text{ and}$$
$$Cu^{2+} > Zn^{2+} > Ni^{2+}.$$
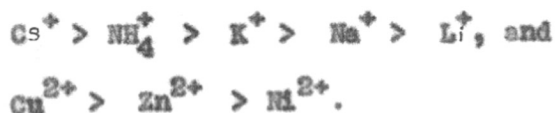
(D) X-ray Diffraction

The X-ray diffraction is a powerful tool for the identification of zeolite species and has been extensively used to understand the kinetics[23,24] and mechanism of zeolite

crystallization. The changes occuring in the lattice parameters on ion exchange, calcination and thermal and hydrothermal treatment of the sample can be also evaluated by the X-ray technique[25].

(E) Infrared Spectroscopy

Infrared spectroscopy has been employed extensively to investigate the framework vibrations[26] in different zeolites and is complimentary to X-ray analysis. The spectra of zeolites in the mid infrared region (200-1300 cm^{-1}) has just like X-ray diffraction, a typical ir pattern for each zeolite. In addition to the framework studies, the ir spectroscopy has been extensively employed for the characterization of surface acidity[27]. The absorption bands at 3600 cm^{-1} and 3720 cm^{-1} correspond to strong and weak Brönsted acid sites respectively. The intensity of the band at 550 cm^{-1} has been related[24] to the crystallinity of the ZSM5 samples.

(F) Thermal Analysis

Thermoanalytical data (DTA, TG, DTG) of zeolites have been extensively used for evaluating the rate of decomposition of occluded organic as well as water molecules from the zeolite cavities. The thermal stability[28] has been estimated from the high temperature exotherm and is related to the Si/Al ratio in the zeolite samples. The weight loss which occurs at about 500°-700°C has been ascribed to the

dehydroxylation of acidic OH groups and the data is used for the estimation of the number of acid sites in the zeolite sample.

(G) Catalytic Reactions over ZSM5 Zeolites

Aromatic hydrocarbons, especially benzene, toluene and xylenes, are important raw materials used in organo-chemical industries. The demand for ortho and para xylenes as chemical intermediates for plastics and polyester fibres has increased rapidly in recent years. Xylenes are produced during reforming of petroleum naptha using the reformer effluent which consists of mainly aromatics and paraffins with very minor amounts of olefins. Xylenes are also produced by catalytic disproportionation of toluene[29] or transalkylation with trimethylbenzene[30], to yield principally xylenes and benzene. Pure ortho xylene is obtained from C_8 aromatic stream by fractional distillation. Because of their close boiling points, p- and meta-xylenes cannot be separated by distillation. But due to relatively high melting point of p-xylene ($+13.3^{\circ}C$) compared with other aromatics, it can be separated by fractional crystallization.

Most of catalytic isomerization studies have been made[31,32] with homogeneous acid halide catalyst. The acidic catalyst such as $AlCl_3$, $AlBr_3HBr$, HF, BF_3 are highly corrosive and suffer from the disadvantage that their hydrogen halide complexes are gases.

On the other hand, vapour phase isomerization over heterogeneous silica-alumina and other duel function catalyst avoids the corrosion and recovery problems but leads to coke formation[33] and lower yield of desired products. Zeolite catalysts are more active than their amorphous counterparts and reach similar conversion levels at lower temperature than that required for the amorphous catalyst[34]. Synthetic zeolites type X, Y and mordenite and ZSM5 have been reported[35] to be good catalysts for isomerization and the selectivities for o, m, p-xylenes can be varied by mere structure modifications. The rare earth exchanged X zeolites had higher activity but side reactions such as disproportionation and cracking reduced[36] the selectivity for isomerization. Due to higher SiO_2/Al_2O_3 ratios the Y zeolites were found to be more stable than the X type. The isomerization activity was related[37] to the acidity of the catalyst and was in the order:

$$HY > REY > MgY > NaY$$

Mordenite catalysts have been extensively studied[38] for isomerization of xylenes both in liquid and vapour phases. However, as a consequence of narrow one-dimensional pores, it was found that during isomerization reaction, the catalyst deactivated by coke deposition.

ZSM5 zeolite is known for unusually high SiO_2/Al_2O_3 ratio and high degree of thermal and acid stability. Xylenes are isomerized[39] at 260-310°C in the absence of hydrogen.

The catalyst is highly selective towards isomerization rather than disproportionation of xylenes[40]. The ratio of isomerization rate (k_i) to disproportionation rate k_d for some of the zeolites are as follows:

Catalyst	k_i/k_d [42]
ZSM5	1000
Mordenite	70
Faujasite	10-20

1.4. SCOPE OF PRESENT WORK

The objectives of this research are two-fold:

(1)   To prepare ZSM5 type zeolites using indigenously available raw materials and to prepare their ion exchanged and acid forms by ion exchange with the appropriate salt solutions and treatment with hydrochloric acid at two different temperatures respectively.

(2)   To study the characteristic properties of the zeolites by X-ray diffraction, thermal analysis, scanning electron microscopy and by selective adsorption of argon, water and hydrocarbons and to correlate the above data with catalytic isomerization of ortho xylene over a few selected samples.

CHAPTER – II

EXPERIMENTAL

2.1. SYNTHESIS OF ZEOLITES

2.1.1. Introduction

The zeolites are generally prepared by using super saturated aqueous solutions of appropriate materials at relatively low temperatures (298 to 473 K). Under these conditions, the nature of the actual product is determined by the composition of the reaction mixture, temperature, reaction period, etc. The synthesis conditions of important zeolites using systems such as $Na_2O-Al_2O_3-SiO_2-H_2O$ have been reviewed[41-43] in detail. Because of lack of thermodynamic equilibrium, there is infinite scope for modifying the reactants and physical conditions to produce new zeolites or to modify the chemical composition (e.g. SiO_2/Al_2O_3 ratio) and physical properties such as size and shape of the crystals.

In typical synthesis, highly unstable reactants, such as "young" coprecipitated gels, in aqueous solution containing an alkali hydroxide at high pH are used. Under such conditions, the zeolite inherits structural units, such as four rings of linked AlO_4 or SiO_4 tetrahedra, with associated cations and water molecules.

Numerous studies have shown that coprecipitated gel undergoes an aging in which the bulk physical nature and consequently intimate atomic linkages change. After this aging process, which presumably produces the appropriate

structural units or building blocks, nucleation and growth
of the zeolite is accomplished from the aqueous phases.
Usually, the aging process is carried out at a lower
temperature (298 K) than the crystallization (373-573 K).

Reactions with smaller changes of entropy favour
zeolites with high disorder. The zeolites with wide pores
and consequent disorder among the water molecules and
exchangeable cations are closer in structural properties and
entropy to the highly disordered gels, and tend to form
initially in preference to the compact zeolites. With
increasing temperature of the synthesis, the more compact
zeolites are formed. The yield of zeolite depends on the
source of the raw materials. Changing the source of SiO_2
from the sodium silicate to colloidal silica produces
marked variations in the products, even for the same bulk
composition and temperature.

Since it is difficult to observe the detailed
atomic movement during the gel formation and crystallization
of zeolites, all theories are speculative, but data on
hydrated cations occuring in the zeolite structure and in-
corporation of various elements like phosphorous by
simultaneous coprecipitation of all components into inter-
mediate gel, support the theories of structural inheritance
during zeolite crystallization.

2.1.2. System for crystallization
of zeolite ZSM5

Increasing attention has been given during the past decade to the synthesis and study of the properties of new zeolite materials crystallized in the presence of organic cations. The synthetic zeolites like the ZSM5 series, will always be most important and great variety of tailor-made species will be possible through the synthesis routes.

The synthesis of ZSM5 zeolite has been reported extensively[44-48]. The system used for the ZSM5 crystallization is

$$(R_4N)_2O - M_2/_nO - Al_2O_3 - SiO_2 - H_2O$$

where $(R_4N)^+$ is the quaternary ammonium cation and M is the alkalimetal cation of valence n. In general, R_4N^+ can be selected from

Tetramethyl ammonium (TMA),

Tetraethyl ammonium (TEA),

Tetrapropyl ammonium (TPA),

triethyl-n-propylammonium (TEPA) and

Tetrabutyl ammonium (TBA),

ions and from the alkalimetal or ammonium cation. Zeolite ZSM5 can be suitably synthesized by preparing a gel containing organic cations, sodium oxide, oxide of aluminium, oxide of silicon and water, having composition in terms of mole ratios of oxides, falling within the range as shown in Table 2.1.

RANGE OF COMPOSITION OF REACTION

MIXTURES IN TERMS OF MOLE RATIOS

OF OXIDES[44]

Ratio	Broad range	Preferred	Particularly preferred
OH^-/SiO_2	0.07-10	0.1-0.8	0.20-0.75
H_2O/OH^-	10-300	10-300	10-300
SiO_2/Al_2O_3	5-100	10-60	10-40
$R^+/(R^+ + Na^+)$	0.2-0.95	0.3-0.9	0.4-0.9

Zeolite ZSM5 is conventionally formed as aluminosilicate.
The composition can be prepared by utilizing materials which
supply the appropriate oxides. Such composition includes for
an aluminosilicates, sodium aluminate, aluminium salts,
alumina, sodium silicates, silica hydrosol, silica gel, silicic
acid, sodium hydroxide and quaternary ammonium compounds. It
has been found that each oxide composition utilized in the
reaction mixture for preparing a member of the ZSM5 family
can be mixed together in any order. Typical reaction condi-
tions consist of heating the reaction mixture, containing
TPABr/TEPABr, Na_2O, Al_2O_3, SiO_2, and H_2O to a temperature of
about 373 to 473 K for a period of about 6 hours to 60 days.
A more preferred temperature is from about 423 to 473 K.
When the temperature is in this range the crystallization
time is reported to be less than 5 days[44]. Crystal size and
crystallization time of ZSM5 will vary with the nature of
the reactants employed.

The factors influencing the synthesis of ZSM5 zeolite using mixed alkyl ammonium cations of the type $R^1_X R^2_Y$ where R^1 and R^2 are different alkyl groups and $X + Y = 4$, have been investigated[48] and results have been compared with the ZSM5 zeolites synthesized in presence of tetrapropyl ammonium $(R_4N)^+$ cations.

In this chapter, the synthesis of ZSM5 using TPABr and TEPABr has been described and the product characterized by XRD, SEM, IR, adsorption and catalytic conversion of ortho xylene.

2.1.3. Synthesis of tetrapropyl ammonium bromide (TPABr)

TPABr was prepared by refluxing equal molar solutions of tripropyl amine (Fluka 99.5% pure) and n-propyl bromide (SDS : 99.5%) in dry ethanol for 24 hours. The excess alcohol was distilled off and the TPABr crystals separated by filtration and washing with dry ethyl ether. The white needle shaped crystals were dried at 363 K overnight in an air oven. The microanalysis of the dry product for C, N and Br agreed with the theoretically calculated values within ± 0.5%.

2.1.4. Synthesis of triethyl n-propyl ammonium bromide (TEPABr)

Triethyl amine, TEA (SDA 99.5%) and n-propyl bromide (SDS 99.5%) were dissolved in methyl ethyl ketone and refluxed at about 363 K for 24 hours on a waterbath.

The TEPABr crystals were separated by filteration, washed
with cold dry ethyl ether and dried at 363 K overnight.
The C, N and Br analysis of the product agreed with the
theoretical values within ± 0.5%.

2.1.5. Synthesis of ZSM5 Zeolites

Synthesis runs were carried out at various
temperatures in stainless steel autoclaves of 75 ml
capacity at autogeneous pressure. The reactants used for
synthesis are given in Table 2.2.

Appropriate amounts of aluminium sulfate and
sulfuric acid were added to distilled water to yield
solution A. Quarternary ammonium compound and sodium
silicate were mixed with water yielding a viscous solution
B. The solution A was added to solution B in reaction
vessel with continuous stirring and then reaction vessel
was sealed as quickly as possible to prevent sorption of
CO_2 from air. The reaction vessels were placed in an air
oven at the required temperature. When the required
temperature was attained (measured with a thermocouple
inserted in a thermowell provided in the autoclave) time was
noted as zeroth hour. On the termination of reaction, the
reactors were quenched in cold water to stop the crystalliza-
tion process. The solid products were filtered, washed with
hot distilled water and dried in static air oven at 393 K for
24 hours.

TABLE - 2.2

SPECIFICATION OF REACTANTS

Chemical name	Chemical formula	Chemical composition
Sodium silicate	Na_2SiO_3	27.2% SiO_2, 8.4% Na_2O, 64.4% H_2O
Aluminium sulphate (BDH)	$Al_2(SO_4)_3.16H_2O$	16.18% Al_2O_3
Sulfuric acid (BDH)	H_2SO_4	98% H_2SO_4
Tetrapropyl ammonium hydroxide (Fluka A.G.)	$(C_3H_7)_4NOH$	40% TPAOH aqueous solution
Tetrapropyl ammonium bromide (synthetic)	$(C_3H_7)_4NBr$	-
Triethyl-n-propyl ammonium bromide (synthetic)	$(C_2H_5)_3C_3H_7NBr$	-

2.1.6. Preparation of HZSM5 zeolites

As synthesized sample of ZSM5 zeolites contain the quaternary ammonium ions and are designated as ZSM5(C/N). The organic quaternary ammonium ions which occupy the channels in the zeolite crystals are removed by heating the sample in a muffle furnace at 813 K for about 8 hours. The final calcination temperature is attained at linear heating rate of 2.5 K min.$^{-1}$. The product is cooled to room temperature and is kept over saturated ammonium chloride solution for a week. The sample is designated as NaZSM5.

In order to obtain NH_4ZSM5, the zeolite samples are exchanged under reflux conditions with 5M solution of NH_4Cl at a liquid to solid ratio of 15:1. The samples are filtered, washed with hot water and dried at 393 K for 12 hours. Same procedure is repeated thrice to obtain maximum exchange.

The acid or protonated forms (HZSM5) are obtained by air calcination of NH_4ZSM5 at 813 K for 8 hours. The heating rate is 2.5 K min^{-1}. Then the sample is cooled to room temperature and kept in a desiccator over saturated ammonium chloride solution for a week. The acid form of the sample is designated as HZSM5. The acid or protonated forms (HZSM5) are also obtained by treating NaZSM5 with 0.973 N HCl. The quantity of acid used is 1 ml/gm of NaZSM5 and 10 ml/gm NaZSM5 respectively.

Both the forms are obtained by stirring the sample in the acid solutions overnight at room temperature and at waterbath temperature respectively.

The samples exchanged at room temperature have been designated as Na-H-(25)-1 and Na-H-(25)-10 where the bracketted figure refers to the temperature of treatment and the numbers 1 and 10 indicate the amount of acid used per gram of the zeolite sample. Similarly, the samples exchanged at waterbath temperature have been designated as Na-H-(98)-1 and Na-H-(98)-10. All the samples are filtered, washed free of excess acid, dried at $120^{o}C$ overnight in an air oven, cooled and kept in a desiccator over saturated ammonium chloride solution for a week.

2.1.7. Cation exchange of NaZSM5

The cation exchanged form of NaZSM5 are obtained by repeated treatment of the NaZSM5 with respective salt solutions using 3-fold excess solution. The relevant data is summarized below. Analytical reagent grade chemicals were used for the cation exchange.

	Sample	Source	Solution used for exchange
1.	Na-K-ZSM5	A.R. BDH	$0.1N$ KCl.
2.	Na-CaZSM5	A.R. BDH	$0.1N$ $CaCl_2$.
3.	Na-MgZSM5	A.R. BDH	$0.1N$ $Mg(NO_3)_2$.
4.	Na-LaZSM5	M/s. Indian Rare Earths, Ltd. Udyogmandal (99.9% purity)	5% $LaCl_3$.
5.	Na-CuZSM5	A.R. BDH	$0.124M$ $Cu(NO_3)_2$.
6.	Na-NiZSM5	A.R. BDH	$0.5N$ $Ni(NO_3)_2$.

All the ion exchanged samples were filtered, washed free of excess cations and dried in an air oven at 120°C overnight, cooled and kept in a desiccator over saturated ammonium chloride solution for a week.

2.2   CHARACTERIZATION OF ZSM5 ZEOLITES

2.2.1. X-ray Diffraction

The synthesized samples were analysed by X-ray powder diffraction method for qualitative and quantitative phase identification. The unit used was Phillips X-ray Diffractometer, Model PW 1730. Ni filtered CuK_α radiation ($\lambda = 1.540$ Å) was used for the analysis of the sample. For quantitative phase identification, selected reference sample was used and per cent crystallization was calculated from the sum of areas of the peaks between $2\theta = 22$ to $25°$. The extent of crystallization was estimated by using the formula[49]

$$\% \text{ Crystallization} = \frac{\text{Peak area between } 2\theta = 22° \text{ to } 25° \text{ of the product}}{\text{Peak area between } 2\theta = 22° \text{ to } 25° \text{ of the reference sample.}}$$

2.2.2. Infrared Spectroscopy

The infrared spectra were recorded in the frequency range 200-1300 cm^{-1} on PYE UNICAM SP 300 Spectrophotometer using KBr pellets and/or nujol mulls of the samples. For quantitative phase identification, a selected reference sample was used and

per cent crystallization was calculated from the area under the peak at 550 cm^{-1}. The extent of crystallization was estimated using the formula[50]

$$\text{\% Crystallization} = \frac{\text{Peak area of the band at } 550 \text{ cm}^{-1} \text{ of the product}}{\text{Peak area of the band at } 550 \text{ cm}^{-1} \text{ of the reference sample.}}$$

KCN was used as an internal standard.

2.2.3. Thermal Analysis

Simultaneous TG-DTA-DTG analyses of intermediate phases were performed on an automatic derivatograph (MOM-Budapest, Type OO-102 B) described by Paulik et al[51]. The thermograms of the samples were recorded under the following conditions:

Weight of the sample	-	70 mgs
Heating rate	-	10 K min^{-1}
Sensitivity		
TG	-	100
DTA	-	1/5
DTG	-	1/5

Preheated and finely powdered ∝-alumina was used as a reference material.

2.2.4. Scanning Electron Microscopy

The morphology of ZSM5 zeolites and representative intermediate phases were investigated by scanning electron microscope, Sterioscan Model 150 Cambridge, U.K. The sample was

dusted on aluminium pegs and coated with an Au-Pd
evaporated film.

2.2.5. Chemical Analysis

Known quantity of zeolite sample was heated at
high temperature in a platinum crucible in duplicate, for
6 hours to constant weight. The dried zeolite powder was
treated with hydrofluoric acid and evaporated to dryness.
The HF treatment was repeated three times. From the loss
in weight silica was estimated. The residue was treated
with hot water and filtered. Some portion of filtrate was
used for estimation of sodium by Flame Photometry. Further,
the residue was treated with potassium pyrosulfate to dis-
solve alumina as well as iron (impurity) as sulfates. This
solution was used to estimate the alumina and iron by
atomic absorption spectroscopy. The per cent composition
of the various samples are given in Table 2.3.

2.2.6. Adsorption of argon, water and hydrocarbons

The adsorption of water and hydrocarbon vapours
in the micropores of ZSM5 zeolites was measured using a
gravimetric quartz spring (McBain) balance shown in Fig.2.1.
The zeolite sample was pressed into a pellet (250 mg) and
activated under a vacuum of 10^{-6} torr at 663 K to desorb
the water from the zeolite pores. After the sample had
reached a constant weight, the temperature of the furnace
was lowered and the sample case was surrounded with a

TABLE - 2.3

CHEMICAL COMPOSITION OF ZSM5 ZEOLITES

WEIGHT PERCENTAGE

Sr.No.	Sample	SiO_2	Al_2O_3	Na_2O	*M_2O	Fe_2O_3
1.	NaZSM5	94.49	4.96	0.44	-	0.33
2.	Na-H-(25)-1	94.73	4.78	0.08	-	0.15
3.	Na-H(25)-10	94.93	4.58	0.011	-	0.154
4.	Na-H-(98)-1	94.92	5.19	0.07	-	0.11
5.	Na-H-(98)-10	94.51	5.00	0.033	-	0.154
6.	Na-K-ZSM5	95.40	5.00	0.03	0.72	-
7.	Na-CaZSM5	96.82	5.08	0.04	0.144	-
8.	NaMgZSM5	97.47	5.11	0.04	0.44	-
9.	NaLaZSM5	95.81	5.03	0.04	1.97	-
10.	Na-Cu-ZSM5	95.97	5.03	0.037	1.76	-
11.	Na-NiZSM5	95.73	5.02	0.051	0.30	-
12.	Na-NH$_4$ZSM5	96.47	5.06	0.019	3.80	-

* M = Exchanged cation.

To high vacuum

To low vacuum

J
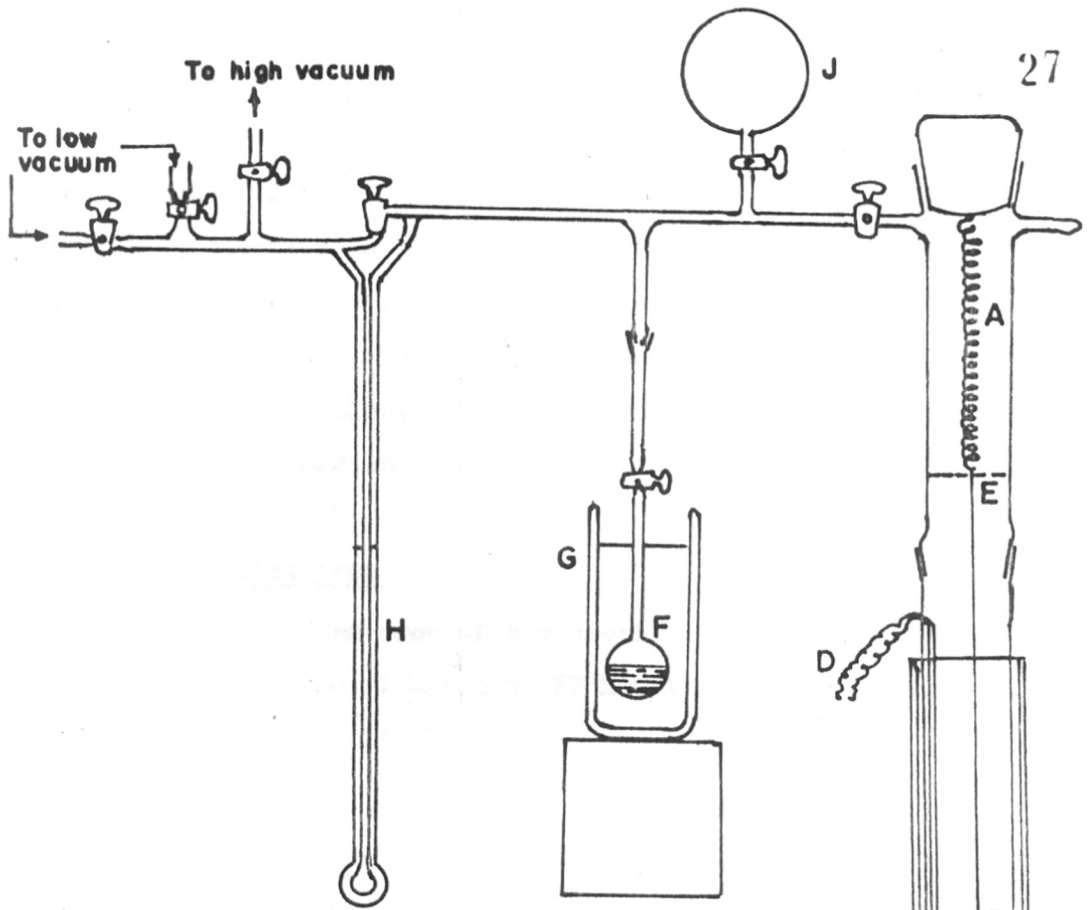
A Silica Spring

B Aluminium Bucket

C Furnace or Thermostat

D Thermocouple

E Reference point

F Liquid bulb

G Thermostat

H Manometer

J Gas Reservoir

FIG.2·1 GRAVIMETRIC ADSORPTION UNIT

thermostat at 298 K. To measure the kinetics and equilibrium adsorption, the sorbate was admitted to the sample and the weight gain by the sample at 298 K was measured as a function of time at constant temperature and pressure. After recording the equilibrium sorption, the sample was evacuated and heated to 653 K at 10^{-6} torr and used for the next measurement.

Surface Area

The surface area of the zeolite samples were determined by the sorption of argon at 77 K using Accusorb Unit (Micromerities Model 2100E).

Surface area determination involved admitting an adsorbate to the sample of known weight, which had been previously activated to make it free of the adsorbed water by heating in vacuum and determining the amount of the sorbate adsorbed by the material, under standard conditions of temperature and pressure.

The surface area is calculated using BET (Brunauer, Emett and Teller) equation :

$$\frac{P}{V_o(P_o - P)} = \frac{1}{V_m C} + \frac{C-1}{V_m C} \; P/P_o$$

where V_o = amount adsorbed at pressure P,

V_m = volume adsorbed when the entire adsorbing surface is covered by a monomolecular layer,

C = a constant, and

P_o = the saturation pressure of the gas.

A plot of $\mathcal{K}$ $P/V_o(P_o-P)$ vs P/P_o gives a straight line, the intercept and slope of which are $\frac{1}{V_m C}$ and $\frac{C-1}{V_m C}$ respectively. From this information and knowledge of the physical dimensions of sorbate molecule, the surface area (SA m^2/g) of adsorbing solid is computed by the following equation

$$SA = \frac{S \times 10^{-20} \times 6.023 \times 10^{23}}{22.414 \times 10^3 \text{ (slope + intercept)}}$$

where S is the area occupied by a single adsorbed gas molecule $(\overset{o}{A})^2.$

2.2.7. Catalytic conversion of ortho xylene over ZSM5 zeolite

The catalytic reactions were carried out in a fixed-bed, down-flow cylindrical silica reactor (Fig.2.2). About 2 gms of the catalyst (10-22 mesh) was positioned in the reactor which was electrically heated. The reactor was provided with a thermowell in the centre for the measurement of the catalyst bed temperature. All the experiments were carried out at atmospheric pressure. Pure ortho xylene was delivered by a metering pump (Model 352, Sage Instrument Co. USA) to a vapourizer, packed with inert porcelain beads. A schematic diagram of the experimental set up is shown in Fig. 2.2   The reaction temperature was maintained constant throughout the catalyst bed.
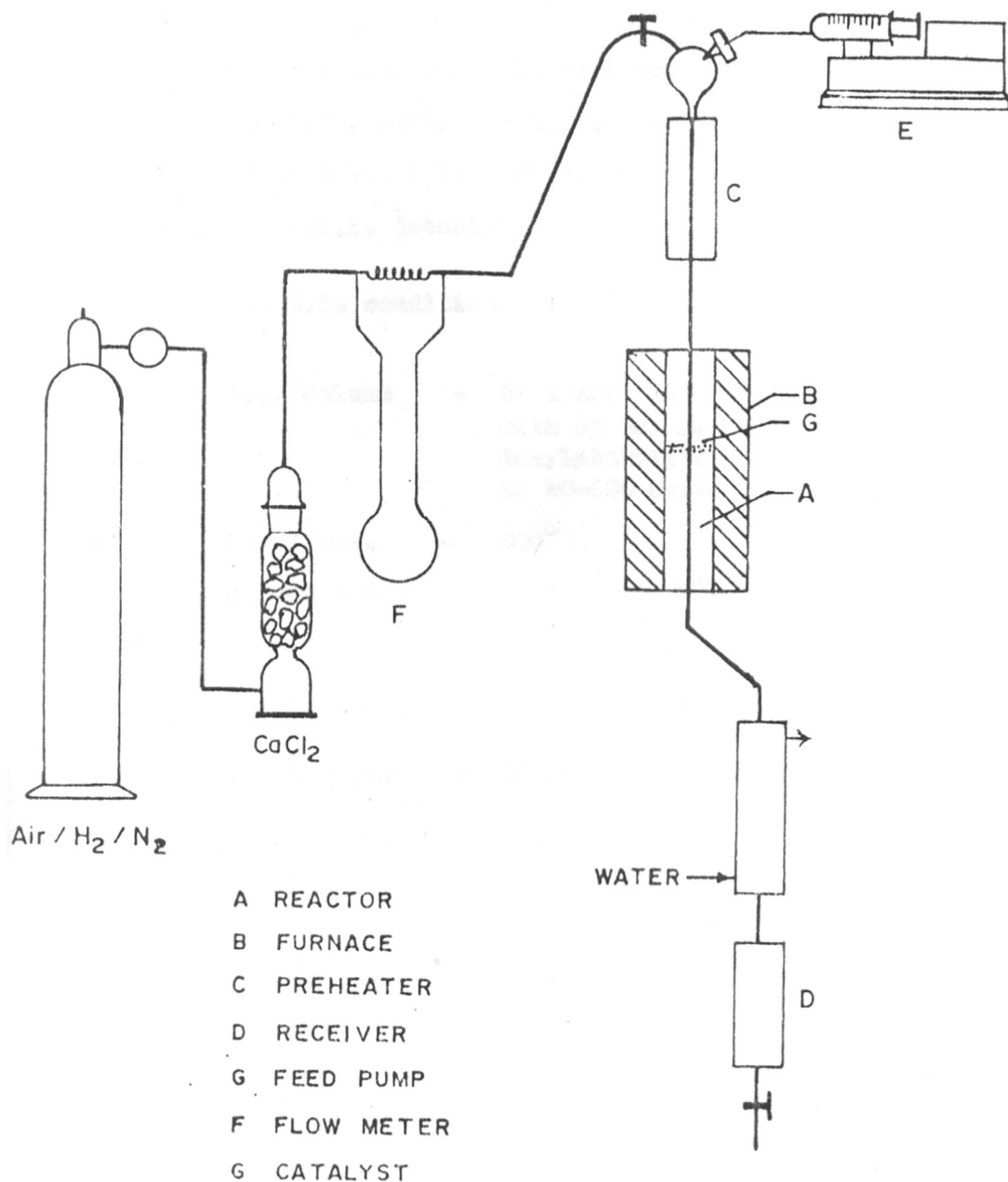
Air / H$_2$ / N$_2$

CaCl$_2$

A   REACTOR

B   FURNACE

C   PREHEATER

D   RECEIVER

G   FEED PUMP

F   FLOW METER

G   CATALYST

WATER

FIG. 2·2   SILICA REACTOR USED FOR ATMOSPHERIC REACTIONS

The reaction products were cooled by passing through condensers, cooled by chilled water and then analysed hourly using a H.P. 5840A gas chromatograph fitted with a F.I.D. detector.

The G.C. conditions are given below:

1.   G.C. Column   -   6' x 1/8" i.d. column packed with 5% bentone + 5% diisodecylphthalate on chromosorb AW 80-100 mesh.

2.   Inj. Temp.   - $200^\circ C$.

3.   Column temp.   -   Isothermal $75^\circ C$ for 5 min. programming at $10^\circ/min.$ to $120^\circ C$ held for 5 min.

4.   F.I.D. temp.   - $250^\circ C$.

5.   Carrier gas   -   Nitrogen, flow rate 200 ml/min.

CHAPTER - III
RESULTS AND DISCUSSION

3.1.   CRYSTALLIZATION OF ZSM5 ZEOLITE

In order to optimise the conditions for obtaining 100% crystalline material, the influence of reaction parameters namely the nature of raw materials, composition, etc. has been studied[48,49,52] extensively. It was observed that the rate of crystallization increases[48] with the SiO_2/Al_2O_3 mole ratio as well as the type of templating agent used in the gel mix. A typical set of experimental results reported are reproduced in Fig.3.1. It was found that increasing the reaction temperature as well as SiO_2/Al_2O_3 strongly enhances the kinetics of the process. Increasing temperature of the reaction mass raises the solubility of the solid aluminosilicate phase which has beneficial effect on the rate of crystallization. Moreover, the observed increase in the rate of crystallization is related to the rate of nucleation of the zeolite phase. The data presented in Fig. 3.1 also indicate that the rate of crystallization is faster in TPABr system rather than TEPABr system.

3.2.   X-RAY DIFFRACTION

The X-ray diffraction patterns of the crystallized products obtained by using TPAOH, TPABr and TEPABr as templating agents are illustrated in Fig. 3.2. The peak height I and the position of the X-ray diffraction peak as
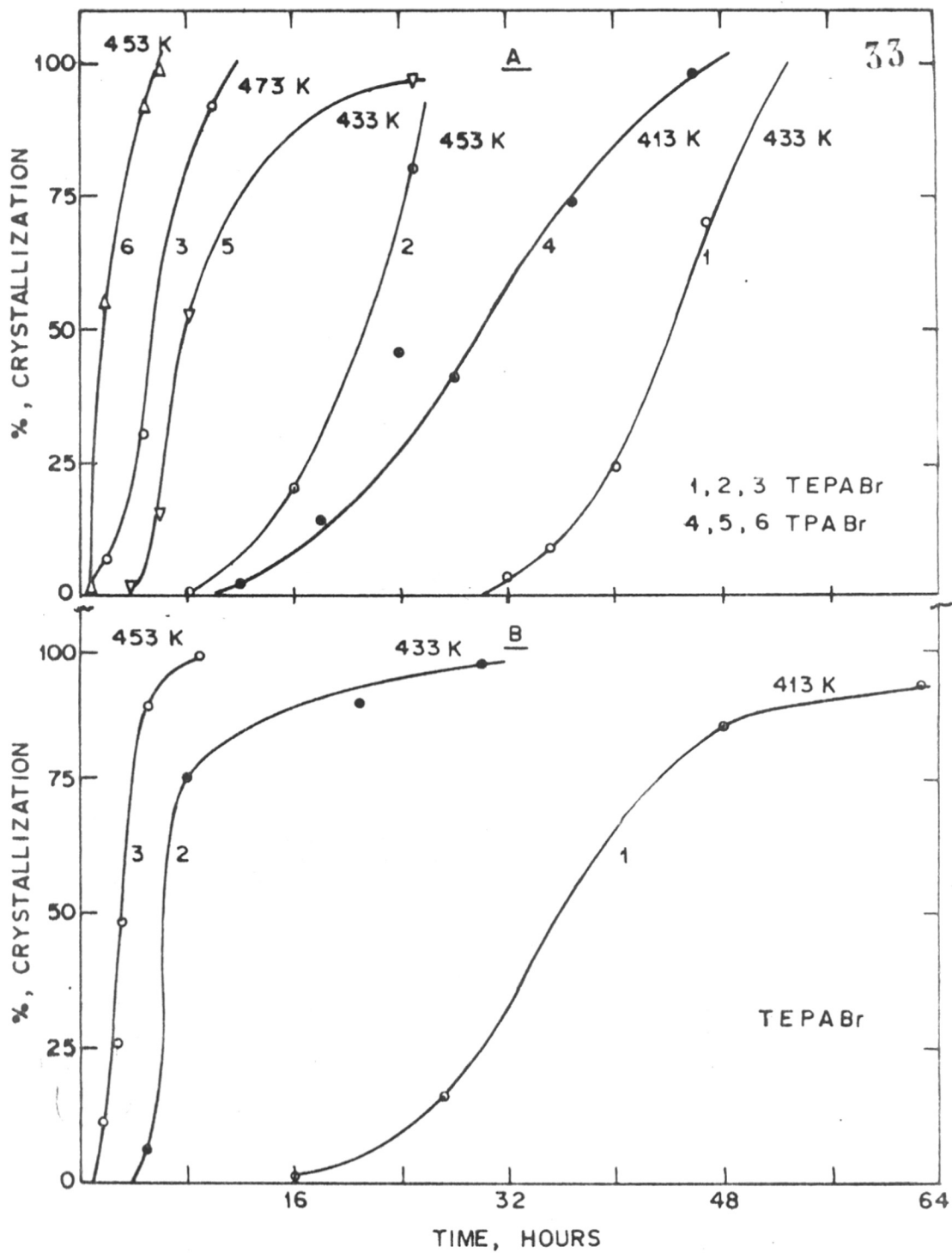
FIG. 3:1. THE KINETICS OF CRYSTALLIZATION OF
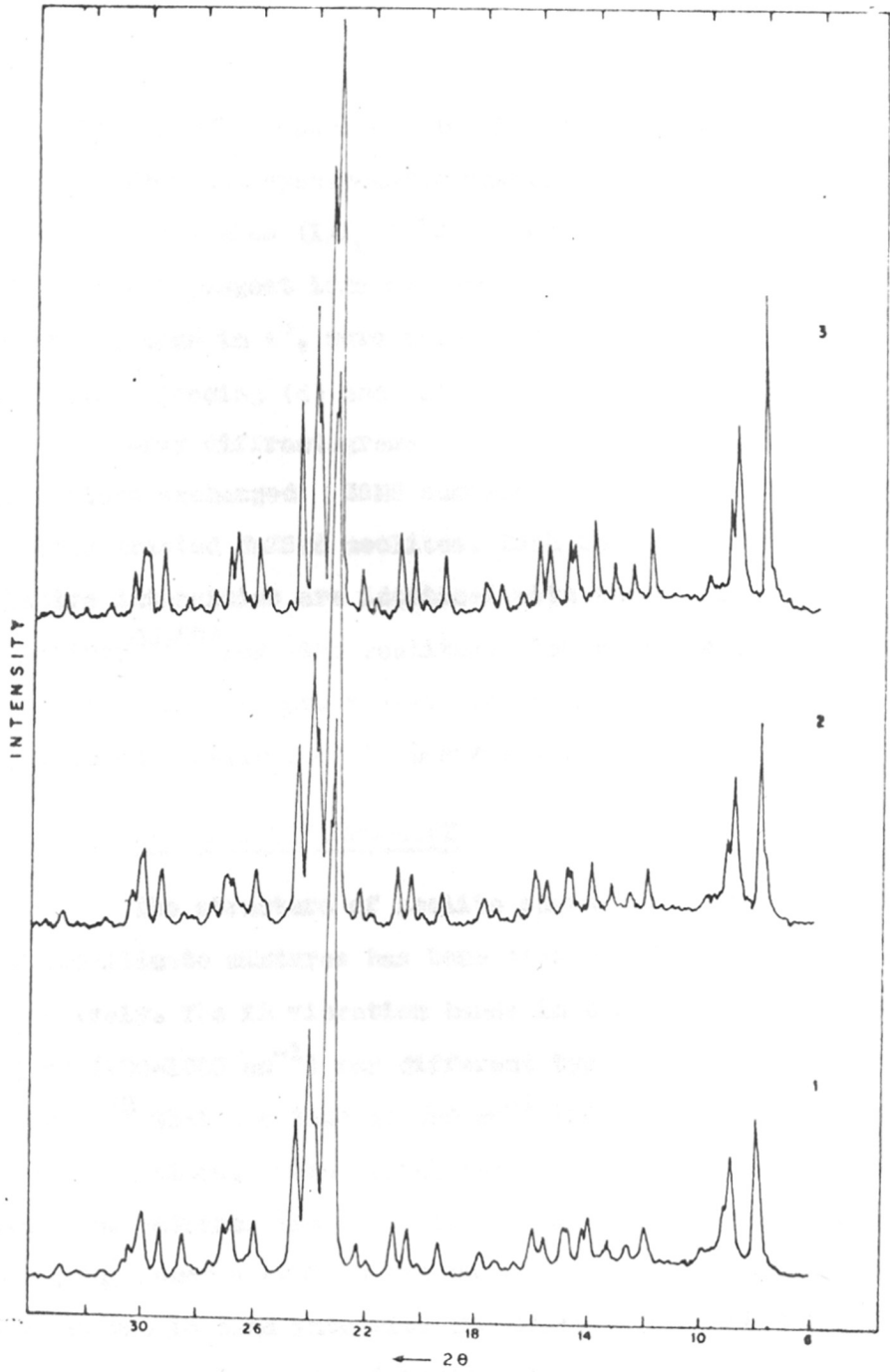A) ZSM-5 ZEOLITE AND B) SILICALITE

FIG. 3·2 X-RAY DIFFRACTION PROFILES OF ZSM-5 ZEOLITES

1) TPAOH   2) TPABr   3) TEPABr

a function of 2θ where θ is the Bragg angle, were estimated from the spectrometer chart. From these, the relative intensities (I/I_o x 100) where I_o is the intensity of the strongest line or peak and d is the interplanar distance in A^o, were calculated. The values of interplanar spacing (d) and relative intensities obtained from the X-ray diffractograms are given in Table 3.1 for the various exchanged ZSM5 samples and Table 3.2 for the acid treated NaZSM5 zeolites. Both the d values and relative intensities are identical with those reported in literature[44,52A] for ZSM5 zeolites. Ion exchange as well as the acid treatment upto nearly one normal HCl does not significantly influence the basic structure.

3.3.   INFRARED SPECTROSCOPY

The structure of zeolite phase formed from the aluminosilicate mixtures has been reported[26,28,50] extensively. The IR vibration bands in the framework region (200-1300 cm^{-1}) for different types of zeolites have shown[50,53] that the band at 550 cm^{-1} indicate the formation of ZSM5 zeolites. Even though X-ray diffraction shows amorphous pattern, the presence of this band unambiguously shows that such a zeolite has been formed. The relationship between the IR band intensity and crystallinity of the sample estimated from the X-ray intensity has been established.

TABLE - 3.1

d-Spacings and relative intensities for

ion-exchanged ZSM5 zeolites

NaZSM5		NaLaZSM5		NaNiZSM5		NaCaZSM5	
$d(A°)$	$(I/I_o) \times 100$	$d(A°)$	$(I/I_o \times 100)$	$d(A°)$	$(I/I_o \times 100)$	$d(A°)$	$(I/I_o \times 100)$
11.11	49.12	10.97	53.57	11.11	48.61	11.04	50.22
10.02	36.40	9.95	32.14	10.04	36.24	10.04	36.12
9.76	13.45	9.81	11.9	9.82	13.86	9.71	13.66
7.43	10.29	7.43	5.95	7.43	7.04	7.43	4.40
6.70	5.26	6.65	5.95	6.70	7.04	6.70	6.16
6.37	7.25	6.32	7.74	6.32	9.80	6.34	8.81
5.98	9.24	5.98	11.90	5.98	11.08	5.98	10.57
5.64	7.60	5.67	8.33	5.67	7.04	5.67	10.23
5.57	8.19	5.53	10.71	5.53	11.51	5.56	8.81
4.62	5.84	4.60	5.36	4.62	7.46	4.62	5.72
4.35	9.36	4.35	9.52	4.37	10.44	4.35	9.69
4.26	10.52	4.24	13.69	4.26	11.30	4.26	11.45
3.86	100	3.83	100	3.86	100	3.86	100
3.81	73.10	3.81	71.42	3.82	69.94	3.82	71.36
3.72	48.54	3.70	47.62	3.75	38.59	3.75	38.60
3.64	28.88	3.64	28.57	3.64	27.50	3.64	28.10
3.48	6.78	3.47	7.14	3.47	7.46	3.47	7.75
3.44	10.99	3.44	10.12	3.44	11.72	3.45	9.52
3.35	8.18	3.34	8.92	3.3	3.34	8.54	6.60
3.04	11.70	3.04	10.71	3.05	13.22	3.05	11.89
2.98	13.10	2.97	11.90	2.97	13.86	2.97	11.45
2.94	6.08	2.94	7.14	2.94	7.25	2.94	6.17
2.60	5.26	2.60	4.76	2.60	6.82	2.60	4.85
2.48	5.84	2.48	5.95	2.48	7.46	2.49	5.73
2.01	9.36	2.00	9.52	2.01	10.66	2.01	9.16
1.99	9.36	1.99	11.30	1.98	11.08	1.99	9.60

TABLE - 3.2

d-Spacings and relative intensities for
acid treated ZSM5 zeolites

Na-H-(25)-1		Na-H-(25)-10		Na-H(98)-1		Na-H-(98)-10	
d(A^o)	(I/I_o x100)	d(A^o)	(I/I_o x100)	(d(A^o)	(I/I_o x100)	d(A^o)	(I/I_o x100)
11.18	49.08	11.07	47.47	11.18	52.33	11.04	41.14
10.04	33.74	9.98	38.05	10.04	37.80	9.92	33.92
9.82	13.74	9.81	15.49	9.82	15.39	-	-
6.32	8.59	6.32	9.56	6.38	9.60	6.32	9.17
5.98	9.82	5.98	12.12	5.96	11.33	5.98	11.71
5.72	6.13	5.67	8.62	5.71	8.99	5.67	8.23
5.57	8.59	5.53	10.10	5.60	17.24	5.53	9.17
4.61	6.13	4.95	5.39	4.61	6.40	4.60	5.56
4.37	9.57	4.59	6.06	4.37	9.24	4.58	5.57
4.26	12.27	4.35	8.08	4.27	11.08	4.24	10.76
4.00	6.44	4.24	11.11	4.00	7.88	3.98	6.33
3.86	100	3.83	100	3.86	100	3.83	100
3.76	33.74	3.70	49.83	3.72	49.26	3.70	46.20
3.65	28.83	3.63	29.63	3.64	28.32	3.63	27.85
3.45	10.06	3.46	7.00	3.48	6.40	3.46	6.33
3.34	8.59	3.34	10.10	3.34	9.24	3.34	8.86
3.31	9.20	3.30	10.77	3.31	10.47	3.30	9.62
3.05	12.26	3.04	12.79	3.06	19.08	3.04	12.66
2.97	13.19	2.96	7.13	2.97	20.32	2.98	13.29
2.93	6.75	2.93	6.40	2.93	7.14	2.93	6.96
2.48	5.21	2.48	6.06	2.49	5.60	2.48	6.65
2.01	8.59	2.02	9.69	2.01	9.98	2.01	10.76
1.90	8.90	1.98	9.16	1.99	9.98	1.90	10.76

The IR spectra of NaZSM5 and acid treated ZSM5 have been recorded (Fig. 3.3) using nujol mull technique and using KCN as an internal standard (reference peak at 2200 cm^{-1}). All the three samples showed strong absorbtion bands in the 400-1200 cm^{-1} region. The band at 1000-1200 has been assigned[26] to internal vibrations of SiO_4, AlO_4 tetrahedra. The absorbance at 550 cm^{-1} has been assigned[54] to highly distorted double 5 membered rings present in the zeolite structure. The area under the peak at this frequency has been employed to estimate[50] the crystallinity of the material. The framework vibration frequencies observed for acid treated NaZSM5 samples are illustrated in Table 3.3. No significant changes are observed in the frequencies of the IR bands.

3.4.   THERMAL ANALYSIS

The zeolite samples synthesized using TPABr as well as TEPABr have been examined by the simultaneous thermal analysis. The loss in weight as well as the thermal effects that occur on heating the sample at a linear heating rate of 10 K min^{-1} have been recorded as the DTA, TG, DTG thermograms and have been employed[54] to estimate the water and organic quaternary ammonium ion content in the crystalline and intermediate phases. The TG curves illustrated in Fig. 3.4 show a two step weight loss at 298-473 K and 523-873 K while the DTA curves shown in Figs. 3.5 and 3.6 exhibit an endotherm at

TABLE - 3.3

Framework vibration frequencies for
ZSM5 type zeolite

Assignment	Wave number observed (cm-1) for sample				
	NaZSM5	Na-H-25-1	Na-H-(25)-10	Na-H-98-1	Na-H-(98)-1
Si-O- bend-ing	460	458	465	460	460
Distorted double 5 rings	560	555	555	550	555
ELC 5	605	-	-	-	-
-	680	680	685	690	685
ITSS	715	715	720	718	720
ELSS	795	800	805	800	808
ELSS	870	890	890	890	890
ITAS	1075	1075	1080	1060	1050
Si-O asym-metric	1220	1230	1230	1230	1230

ELC5 - External Link Complex Five Membered ring;

ELSS - External Link Symmetric Stretch;

ITSS - Internal Tetrahedral Symmetric Stretch;

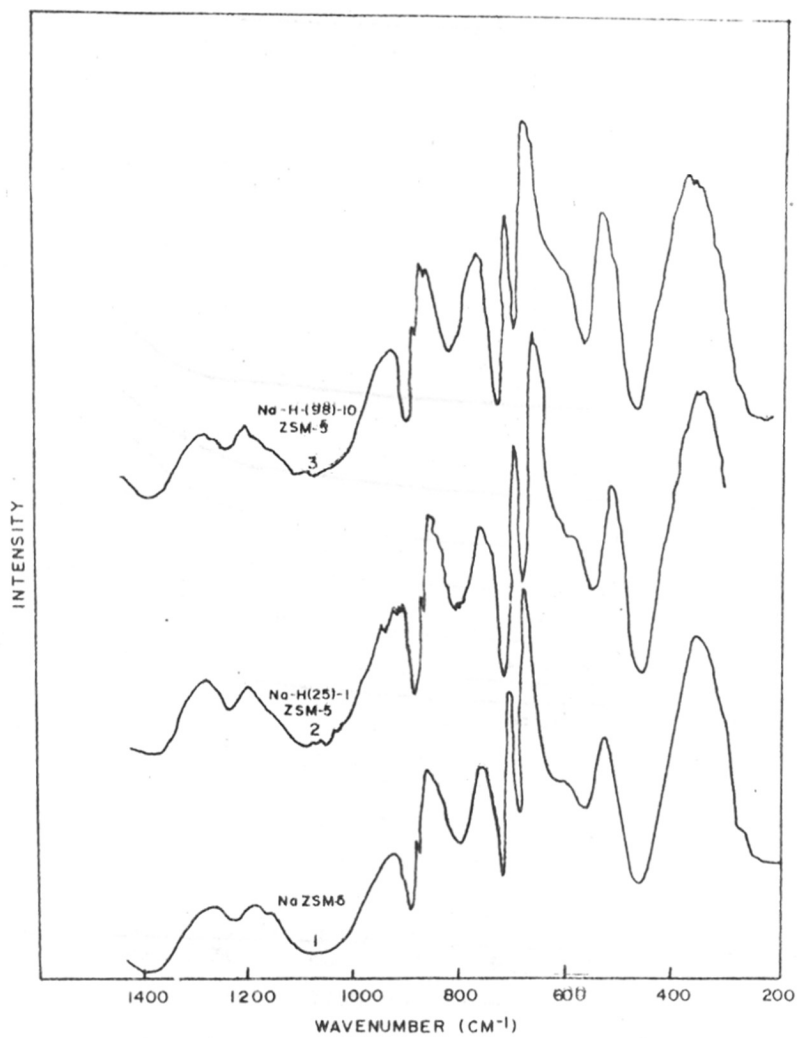ITAS - Internal Tetrahedral Asymmetric Stretch.

INTENSITY

Na-H-(98)-10
ZSM-5
3

Na-H(25)-1
ZSM-5
2

Na ZSM5
1

1400   1200   1000   800   600   400   200

WAVENUMBER (CM⁻¹)

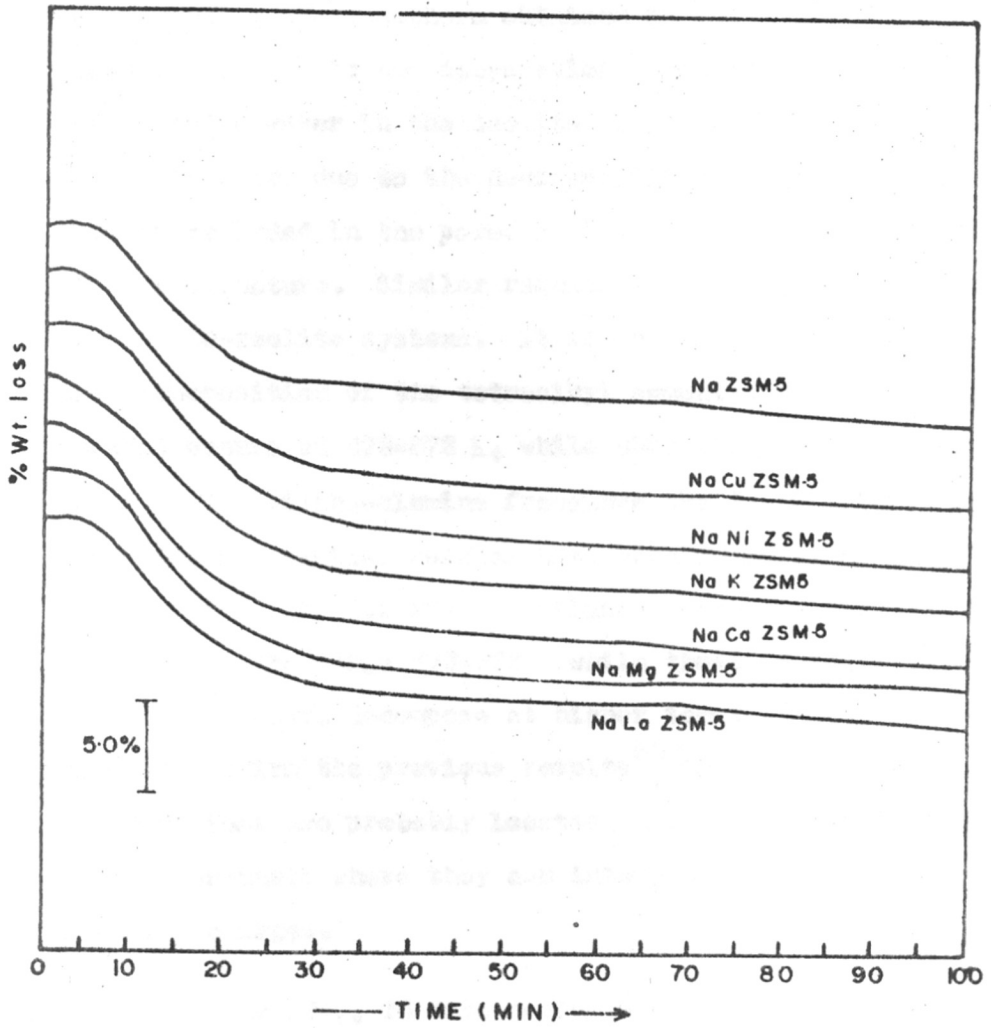FIG 3·3 I R SPECTRA OF ZSM-5 TYPE ZEOLITES

FIG 3·4 TGA OF ZSM-5 TYPE ZEOLITES

298-473 K and exotherms with three peaks between 573 to 873 K respectively. The endotherm obtained in the temperature range 298-473 K is due to the dehydration of physically adsorbed and occluded water in the zeolite, while the exotherms (523-873 K) are due to the decomposition of the organic cations occluded in the pores of the zeolite during synthesis of ZSM5 structure. Similar results have been obtained for the TPABr-zeolite systems. It is interesting to note that the decomposition of the tetraalkyl ammonium salts (TPABr/ TPABr) occurs at 473-573 K, while when these cations are bound to the silica-alumina framework the decomposition occurs above 623 K. Similar results have been reported by Manton and Davidtz[55] in case of TPA cations. Pure TPA decomposes in the temperature range 473-573 while those occluded in the zeolite framework decompose at higher temperatures. These results confirm the previous results[56] that the quaternary ammonium ions are probably located at the intersections of the zeolite channels where they can interact with the framework negative charges.

The DTA,, TG data evaluated from Figs. 3.4 to 3.6 for the various ion exchanged and acid treated ZSM5 zeolites show that while complete dehydration occurs between 298 to 543 K for the original NaZSM5, on ion exchange with di- and trivalent cations, complete dehydration takes place at much higher
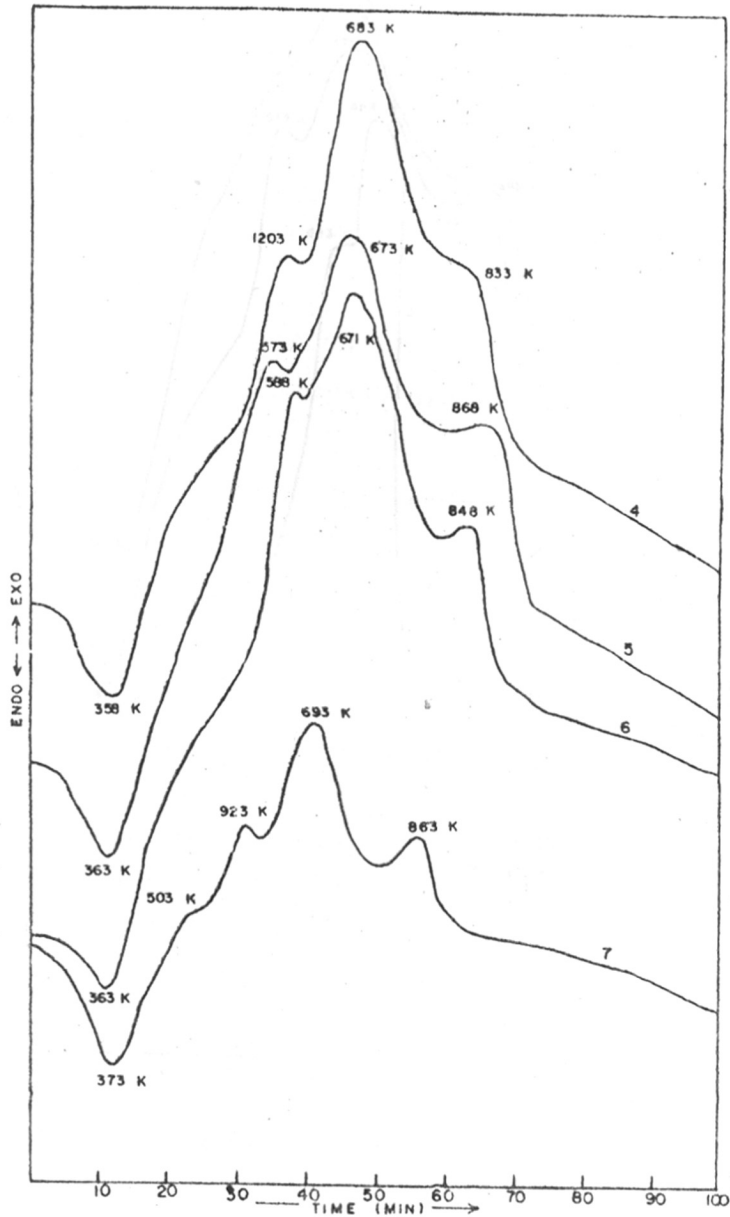
FIG 3·5 DTA OF ZSM·5 TYPE ZEOLITES

Curves 4: Na-NH₄-ZSM5   5: Na-H-(25)-1-ZSM5
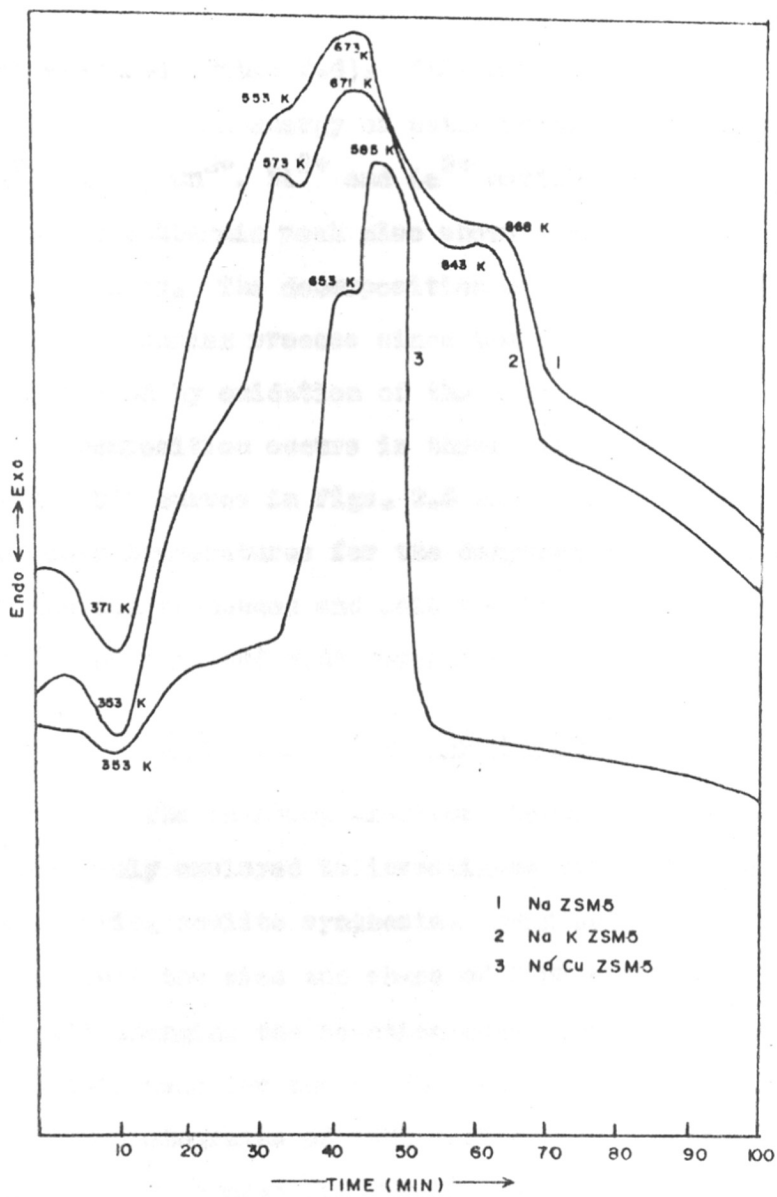   6: Na-La-ZSM5   7: Na-H-(25)-10-ZSM5

FIG 3·6 DTA OF ZSM—5 TYPE ZEOLITES

Endo ←→ Exo

673 K
671 K
553 K
573 K
585 K
866 K
653 K
843 K
371 K
353 K
353 K

3   2   1

1   Na ZSM5
2   Na K ZSM5
3   Nd Cu ZSM5

TIME (MIN)

10   20   30   40   50   60   70   80   90   100

temperatures (Table 3.4). This may be ascribed to the
higher hydration energy of water molecules bound to
Mg^{2+}, Ca^{2+}, Cu^{2+}, Ni^{2+} and La^{3+} cations. The minimum
of the endothermic peak also shows a shift to higher
temperatures. The decomposition of quaternary ammonium
ion is a complex process since the decomposition is
accompanied by oxidation of the decomposition products.
The decomposition occurs in three stages as illustrated
by the DTA curves in Figs. 3.5 and 3.6. The weight loss
and peak temperatures for the dehydration and decomposition
of the ion exchanged and acid treated ZSM5 samples are given
in Tables 3.4A and 3.4B respectively.

3.5. SCANNING ELECTRON MICROSCOPY

The scanning electron microscopy (SEM) has been
extensively employed to investigate morphological characteris-
tics during zeolite synthesis. Sand and coworkers[57] have
shown that the size and shape of ZSM5 crystals can be altered
at will changing the reaction conditions as well as raw
materials used for the synthesis. In a limited application
the SEM photographs of ZSM5 zeolite and representative
intermediate phases for TPABr system ($SiO_2/Al_2O_3 = 86$,
$OH/H_2O = 5.8 \times 10^{-3}$, T = 453 K) are shown in Fig. 3.7. The
photographs A and B indicate amorphous gel and coexistance
of both amorphous and crystalline phases respectively after

TABLE - 3.4A

DTA and TG data for cation exchanged

ZSM5 zeolites

Zeolite	% Exchange	% Loss in wt.	Temperature(°K) of	
			Minimum of endothermic peak	Complete dehydration
NaZSM5	-	8.5	373	543
NaKZSM5	93.18	11.0	413	663
NaCaZSM5	90.9	11.0	398	713
NaCuZSM5	91.60	11.0	383	608
NaLaZSM5	90.9	9.5	362	673
NaMgZSM5	90.9	11.0	373	743
NaNiZSM5	88.40	11.0	383	636

TABLE - 3.4 B

DTA data for ion exchanged samples

Sample	Peak temp. in °K		
	Ist Peak	IInd Peak	III Peak
NaZSM5	653	673	868
Na-K-ZSM5	573	671	843
Na-Cu-ZSM5	653	625	-
Na-NH$_4$-ZSM5	1203	683	833
Na-H-(25)-1	573	673	868
Na-La-ZSM5	588	671	848
Na-H-(25)-10	923	693	863
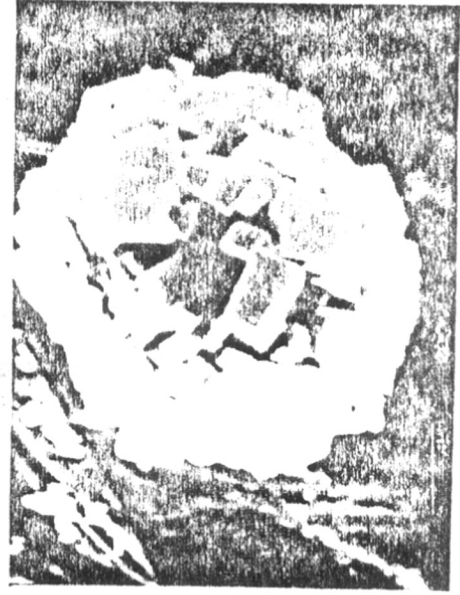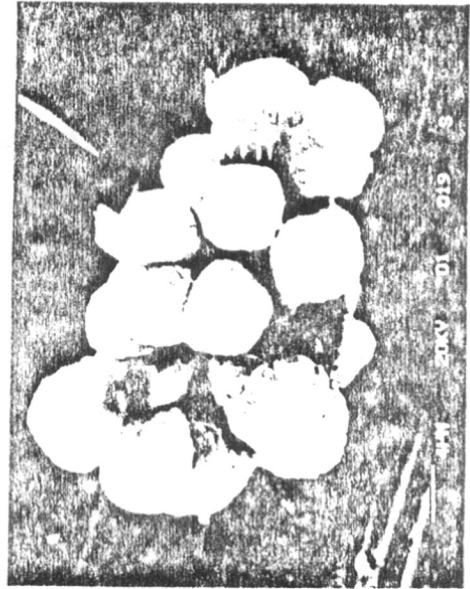
FIG 3.7 SEM PHOTOGRAPHS OF ZSM-5 AND INTERMEDIATE PHAGES
A) AMORPHOUS B) 15%CRYSTALLINE C) 75%CRYSTALLINE D)100% CRYSTALLINE

16 hours of crystallization at 453 K. The presence of
amorphous material at higher crystallization period indicates
that crystalline phase is embeded in the amorphous material.
Similar results were obtained in the systems where TPABr was
used as a templating agent. The morphology and crystallite
size are similar in both TPABr and TEPABr systems. Fig. 3.7C
and D show the micrographs of fully crystalline material and
blown up picture of one polycrystalline aggregate of about
16-20 µm.

3.6.   ADSORPTION

The adsorption and catalytic properties of zeolites
are modified[58] to a considerable extent by the replacement of
Na$^+$ in the original zeolite with hydrogen or other multivalent
cations. The changes in the properties of zeolite brought
about by ion exchange are usually determined by the variations
in the sorption, thermal and acidic properties. The low tempera-
ture nitrogen and argon adsorption isotherms for pure zeolite
sample is quite characteristic and is distinguishable from that
of the amorphous materials. Nitrogen adsorption isotherms have
been employed to estimate[59] the per cent crystallinity of the
synthetic and thermally treated zeolite catalysts. Moreover,
such isotherms are used[60] for the calculations of the surface
accessible to molecules comparable in size and also the surface
area of the samples. From the sorption capacities of water,
n-hexane and cyclohexane, the modifications in the pore
structure of the zeolite can be determined and the total pore

volume estimated. Similarly, the sorption data for the reactant molecules and products formed during the reaction namely ortho- meta- and p-xylenes in the catalyst samples provided useful correlation for the activity of the catalyst. The adsorption of hydrocarbon molecules of varying sizes and shape as well as those of reactants and products formed during xylene isomeri- zation are presented in the following sections.

(A) Adsorption of argon

The sorption data at 77°K are summarized in Tables 3.5 and 3.6. The values of V_m and surface areas have been estimated by the application of BET equation described in Chapter II. The adsorption isotherms for argon at 77°K are illustrated in Fig. 3.8 and the BET plots are shown in Figs. 3.9 and 3.10 respectively. The surface areas estimated from the BET plots show an increase from about 364.7 m^2/g for NaZSM5 to 412 m^2/g for the acid extracted sample NaHZSM5(25). Similar changes are observed in the equilibrium adsorption volumes V_m (Tables 3.5-3.7). However, the values of pore volume V_p estimated by the application of Dubinin equation do not vary significantly in the various samples. The Dubinin plots log a Vs $[\log P_o/P]^2$ shown in Fig. 3.11 have been employed to evaluate the value of 'a' and the total pore volume of the sample.

The sorption capacity for argon follows the order
NaH(25) > NaH(98)-10 > NaLaZSM5 > NaZSM5.
It may be observed from Table that NaH(98)-10 and NaHZSM5

TABLE - 3.5

ADSORPTION OF ARGON AND SURFACE

AREAS OF ZSM5 ZEOLITES

Sample	Sorption equilibrium V_m (ccs/gm)	Surface area (M^2/gm)
Na-ZSM5	98	364.7
Na-H-(98)-10-ZSM5	103.5	383.5
Na-La-ZSM5	102	381.00
Na-H-(25)-10-ZSM5	108.9	412.00

TABLE - 3.6

VOID VOLUME OF ION EXCHANGED

ZSM5 TYPE ZEOLITE

Zeolite	$\log a_s$	a_s (ccs/gm)	a_s (gms/gm)	V_p (ccs/gm)
NaZSM5	2.125	133.35	0.24	0.171
Na-H-(98)-10 ZSM5	2.063	115.611	0.21	0.15
NaLaZSM5	2.06	113.71	0.203	0.145
Na-H-(25)-10 ZSM5	2.09	123.03	0.22	0.16

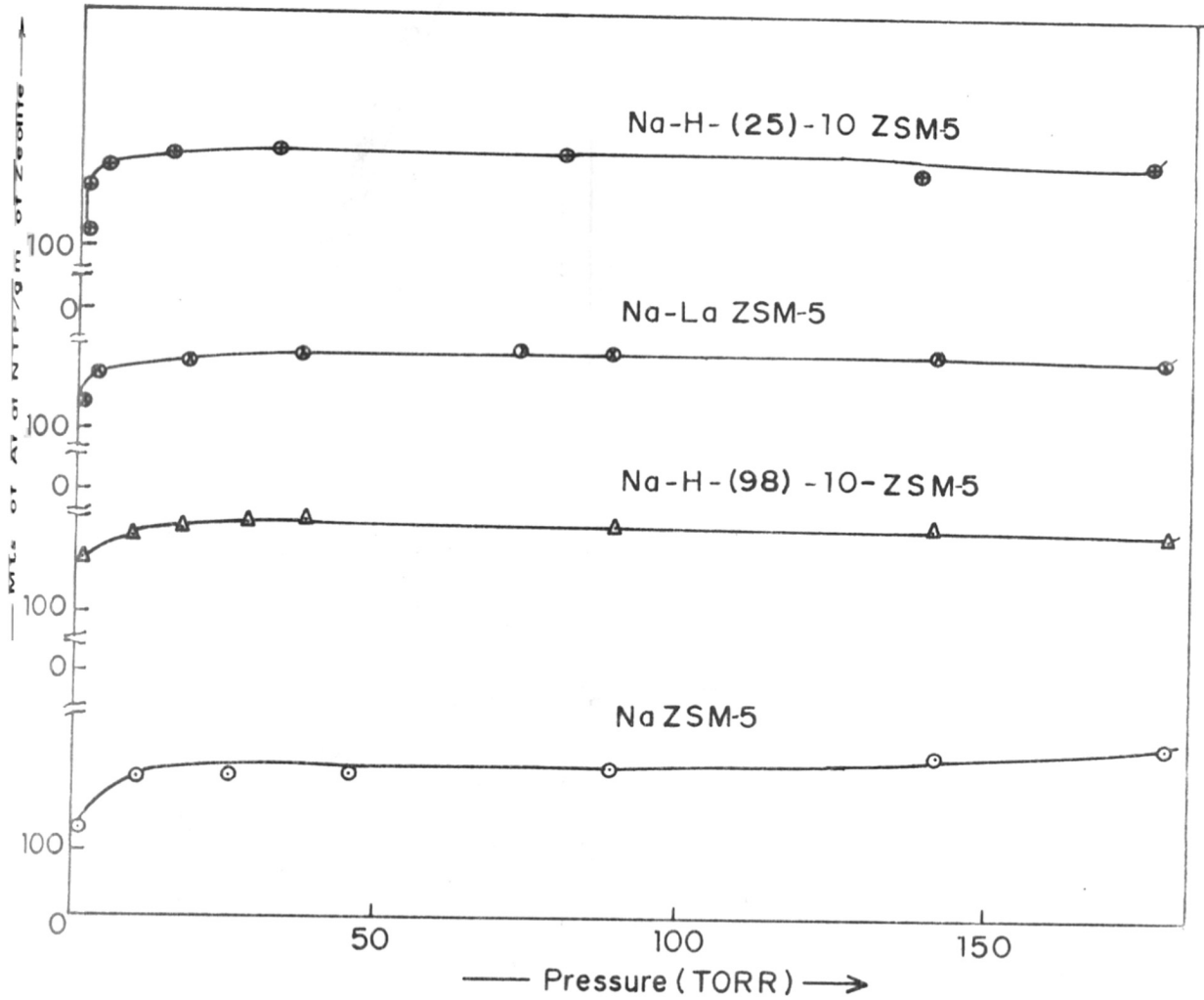a_s = saturation capacity,

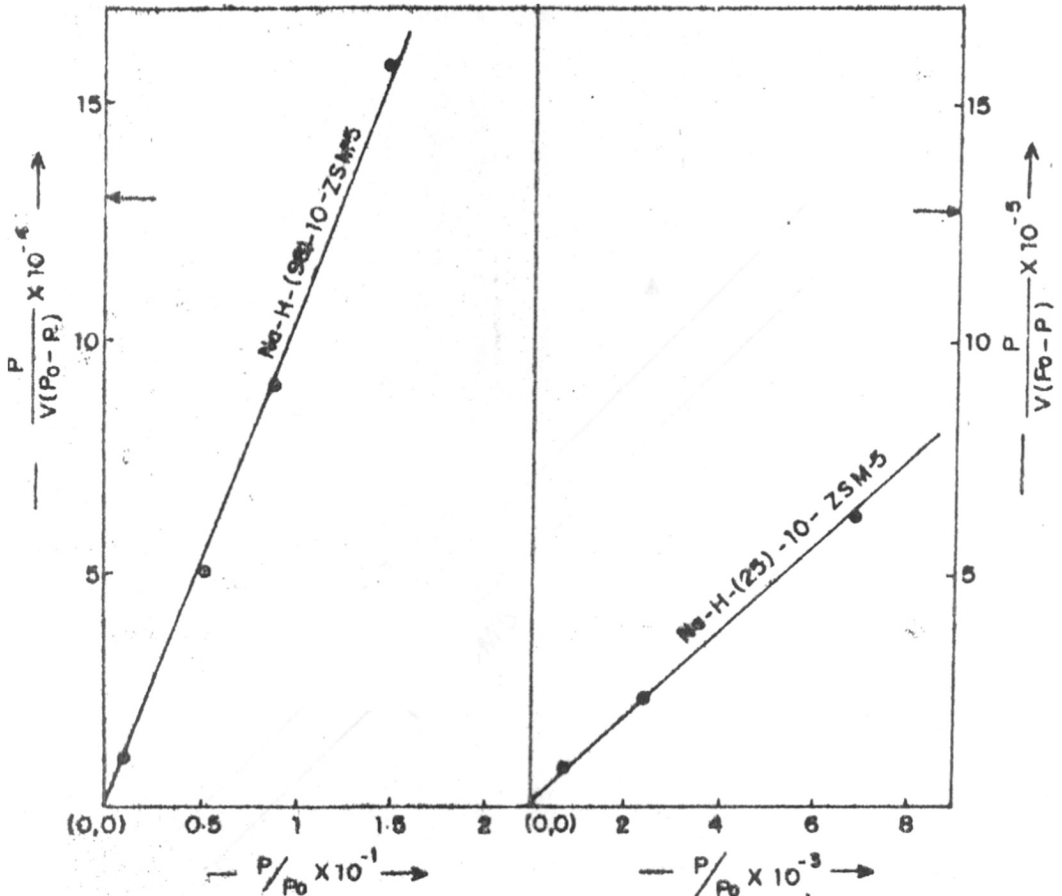V_p = total void volume.

FIG. 3.8 ADSORPTION OF ARGON ON ZSM-5 TYPE ZEOLITES

FIG. 3.9 B.E.T. PLOTS FOR ZSM-5 ZEOLITE (Argon - adsorption at 77 K)
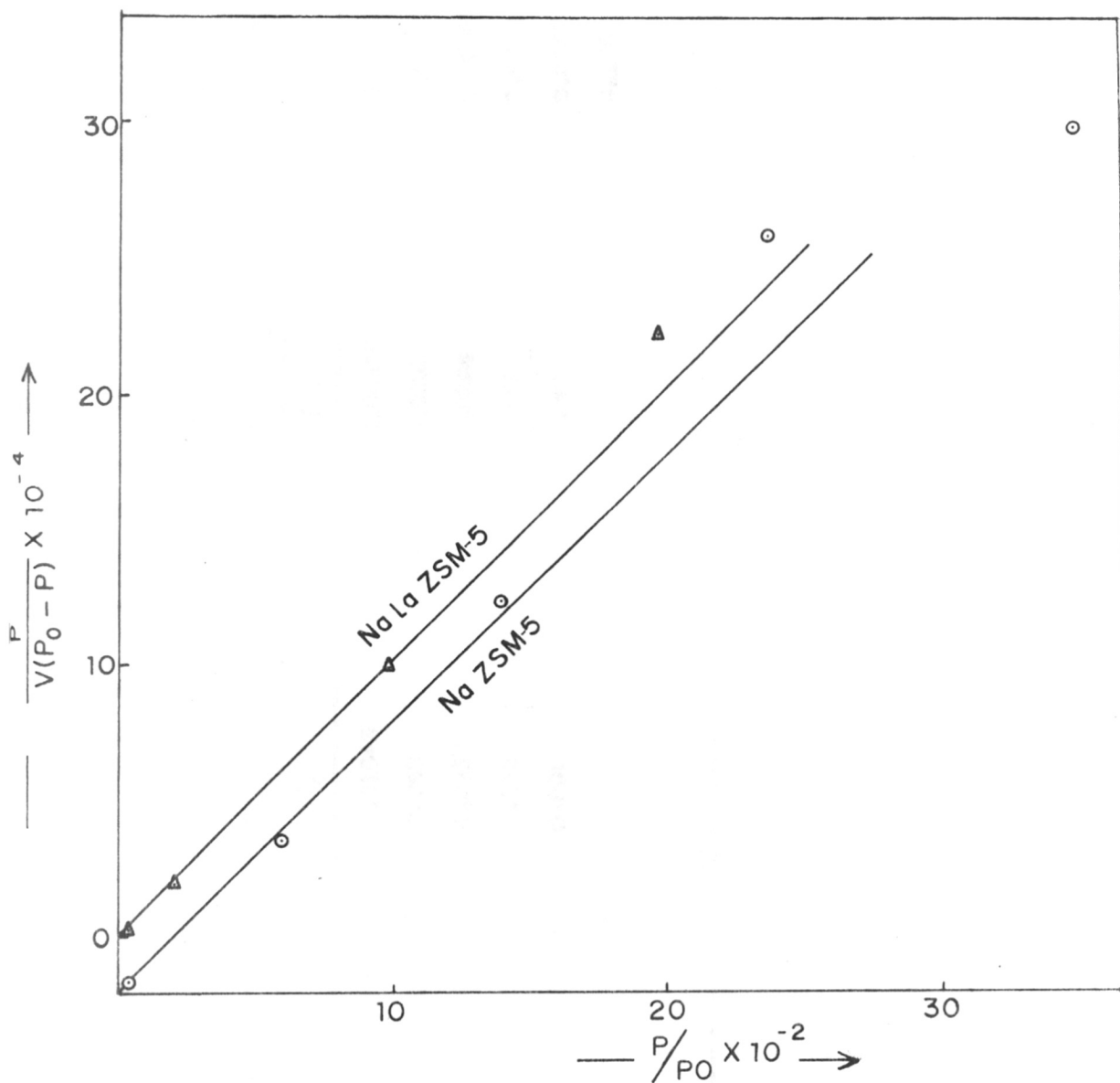
FIG. 3·10 B.E.T. PLOTS FOR ZSM-5 ZEOLITES(Argon - adsorption at 77 K)

TABLE - 3.7

ΔG° VALUES FOR ZEOLITE - AT SYSTEM AT 77°K

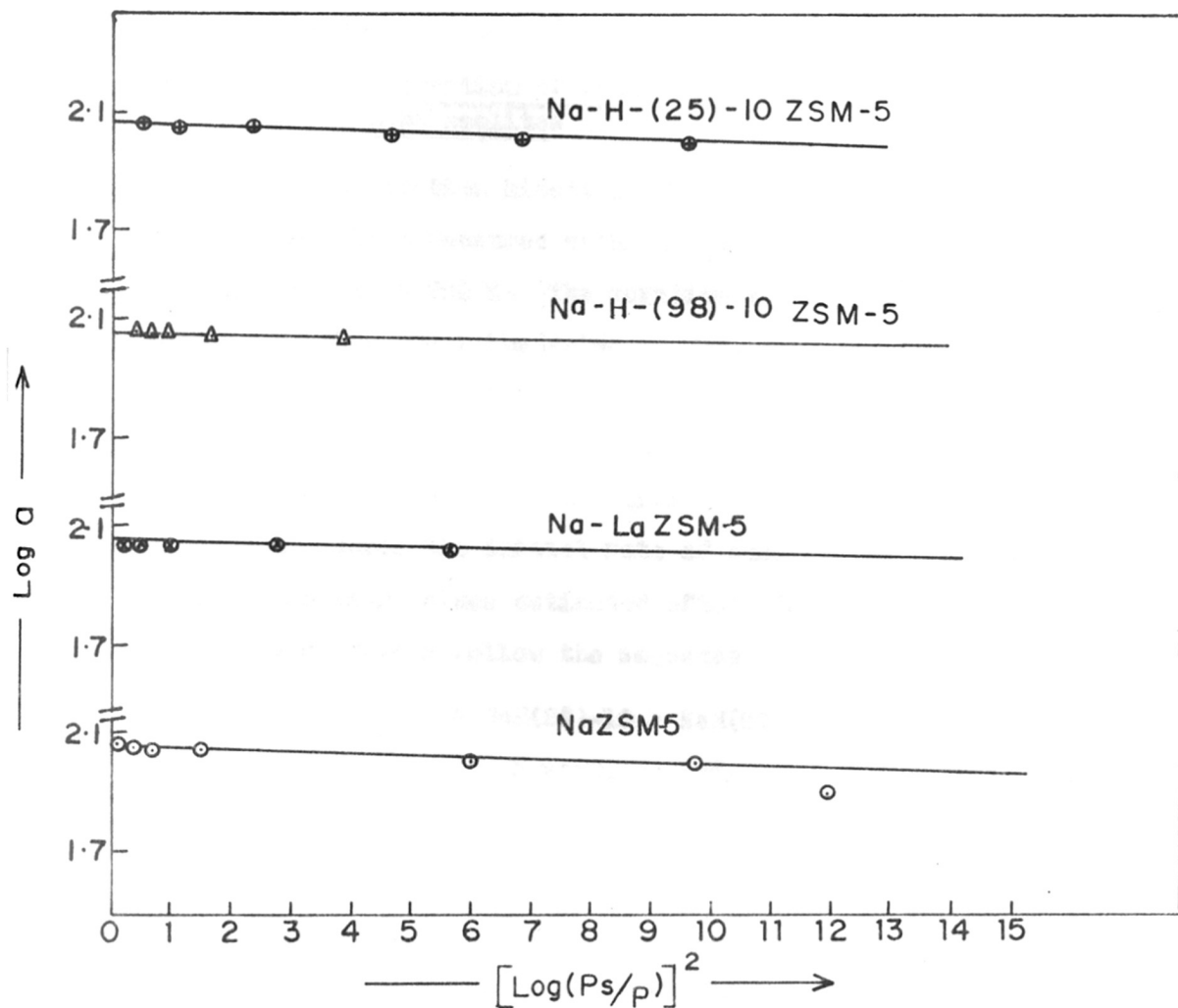| Na-ZSM5		Na-H-(98)-10-ZSM5		Na-La-ZSM5		Na-H-(25)-10-ZSM5	
P/P_0	$\Delta G°$ cals/mole	P/P_0	$\Delta G°$ cals/mole	P/P_0	$\Delta G°$ cals/mole	P/P_0	$\Delta G°$ cals/mole
0.00077	1093	0.01043	695.69	0.00419	834.73	0.0007582	1095.36
0.0035	582.16	0.052	460.75	0.0209	589.72	0.002391	920.25
0.059	431.50	0.0938	361.63	0.0994	351.97	0.006860	759.12
0.14	299.58	0.152	287.21	0.200	245.38	0.0288	543.50
0.47	115.11	0.201	244.61	0.383	144.34	0.0836	378.54
0.75	43.86					0.175	265.73
0.94	9.43						

FIG. 3·11 DUBININ PLOTS FOR THE ADSORPTION OF ARGON ON ZSM-5 TYPE ZEOLITES

contain 0.0412 and 0.072 Na$^+$ ions per unit cell. The equilibrium sorption capacity of the zeolite sample is found to increase with decreasing Na$^+$ ions per unit cell. The free energy of sorption ΔG^0 ($-$ RT ln P_0/P) is given in Table 3.7.

(B) Adsorption of water vapour on ZSM5 zeolites

The sorption kinetics of water vapour on ZSM5 samples have been measured using a gravimetric McBain silica spring balance at 298 K. The sorption kinetics for the acid treated samples are illustrated in Fig. 3.12 and for the cation exchanged zeolites in Fig. 3.13. It can be seen that the initial rate of sorption is more for the original NaZSM5 samples (Fig. 3.12). Acid treatment and ammonium exchange appears to reduce the initial rate of adsorption. The equilibrium adsorption values estimated after 120 minutes exposure to the water vapour follow the sequence

NaZSM5 > NaH(98)-10 > NaH(25)-10 > NaH(98)-1 > NaH(25)-1

> NaNH$_4$(H)ZSM5.
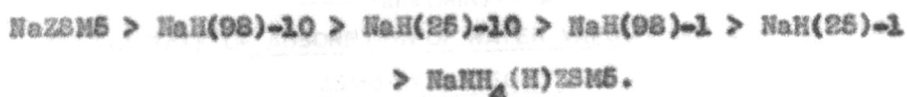
These results indicate some lattice distortion and increasing order of hydrophobicity in the above samples has taken place on acid treatment of the ZSM5. The cation exchanged ZSM5 zeolites indicate marked changes in the sorption of water (Fig. 3.13). While the H$_2$O sorption increases on K$^+$ and Ni^{2+}
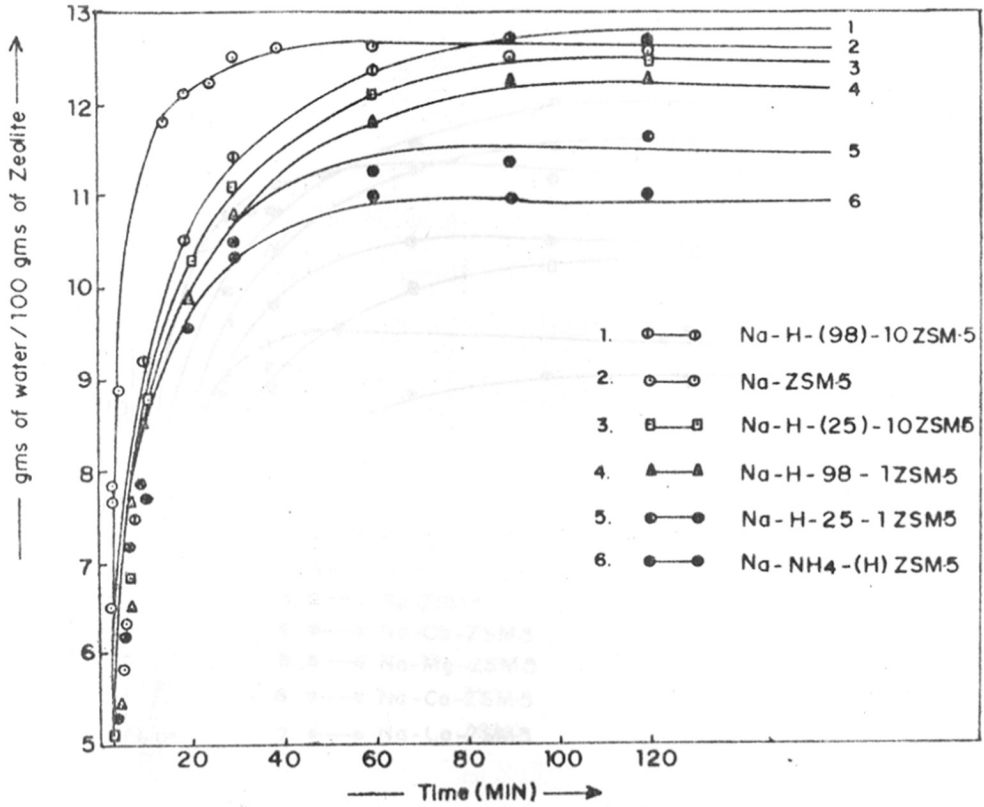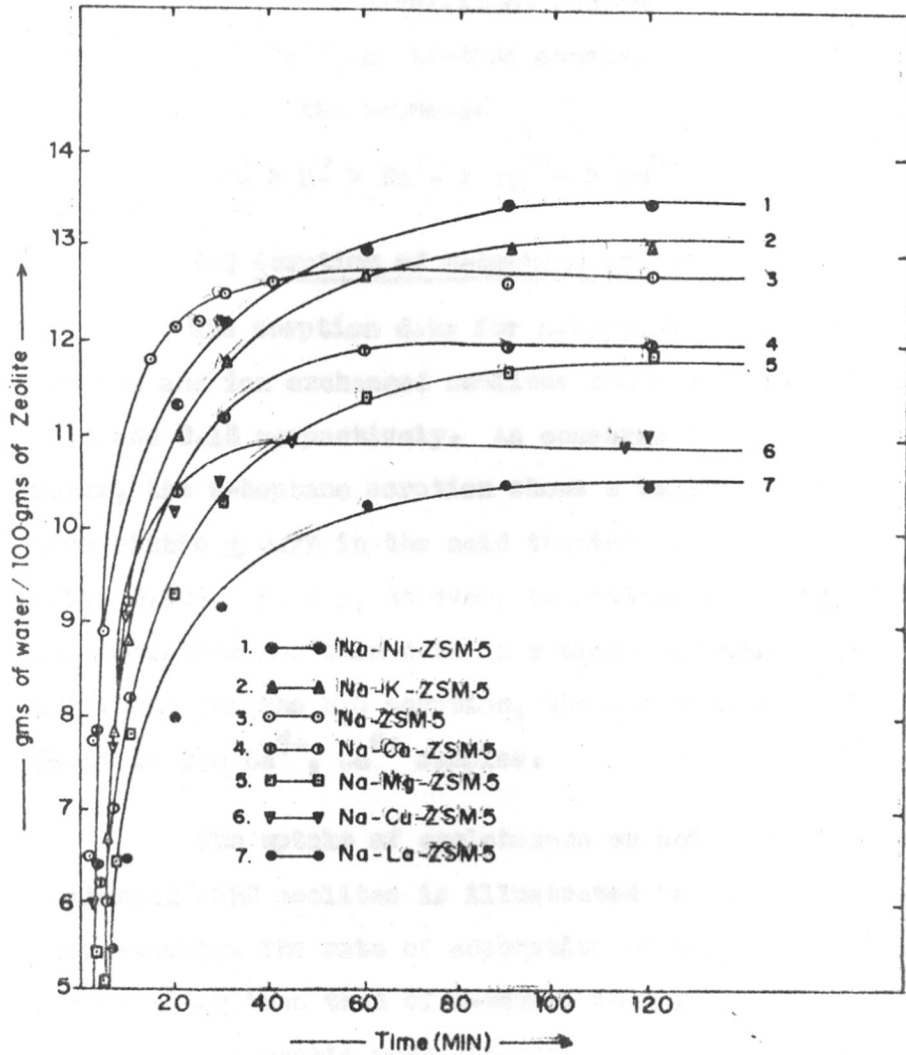
FIG.3·12 RATE OF ADSORPTION OF WATER VAPOUR ON ACID TREATED ZSM5 TYPE ZEOLITES

FIG.3.13 RATE OF ADSORPTION OF WATER VAPOUR ON CATION EXCHANGED ZSM-5 TYPE ZEOLITES

exchange, there is a significant decrease in H_2O sorption in Ca^{2+}, Mg^{2+}, Cu^{2+} and La-ZSM5 sample. The sorption capacity follows the sequence

$$Ni^{2+} > K^+ > Na^+ > Mg^{2+} > Cu^{2+} \rightarrow La^{3+} ZSM5.$$

(C) Sorption of n-heptane and cyclohexane

The sorption data for n-heptane in different acid treated and ion exchanged zeolites are illustrated in Fig. 3.14 and 3.15 respectively. As compared to the sorption of water, the n-heptane sorption shows a relatively small variation within $\pm 0.7\%$ in the acid treated H-form of the ZSM5 (Fig. 3.14). It may, however, be noticed from Fig. 3.15 that the n-heptane sorption data in cation exchanged forms follows the trend for the H_2O sorption, the sorption of heptane being least in the La^{3+}, Ca^{2+} samples.

The uptake of cyclohexane on acid treated and ion exchanged ZSM5 zeolites is illustrated in Fig. 3.16 and 3.17 respectively. The rate of adsorption of cyclohexane is very much smaller than that of n-hexane in a given zeolite sample. The crystallographic pore dimensions of ZSM5 catalyst (5.4 x 5.6 A) cannot be used to estimate precisely what molecules will be sorbed and what molecules excluded. While decrease in adsorption of water and hexane corresponds to general expectation, the decrease in the rate of cyclohexane adsorption with acid treatment is surprising. In general, the rate of sorption of cyclohexane in ZSM5 samples is slow and equilibrium is not
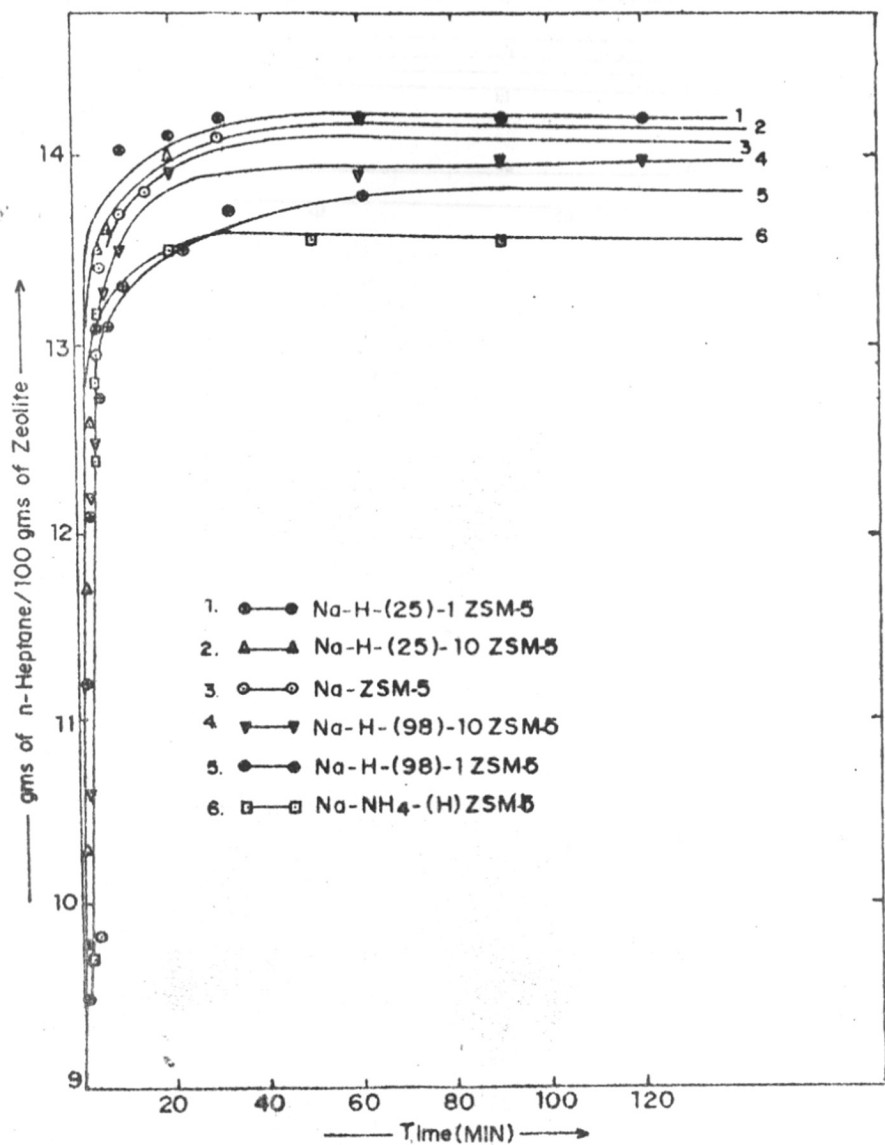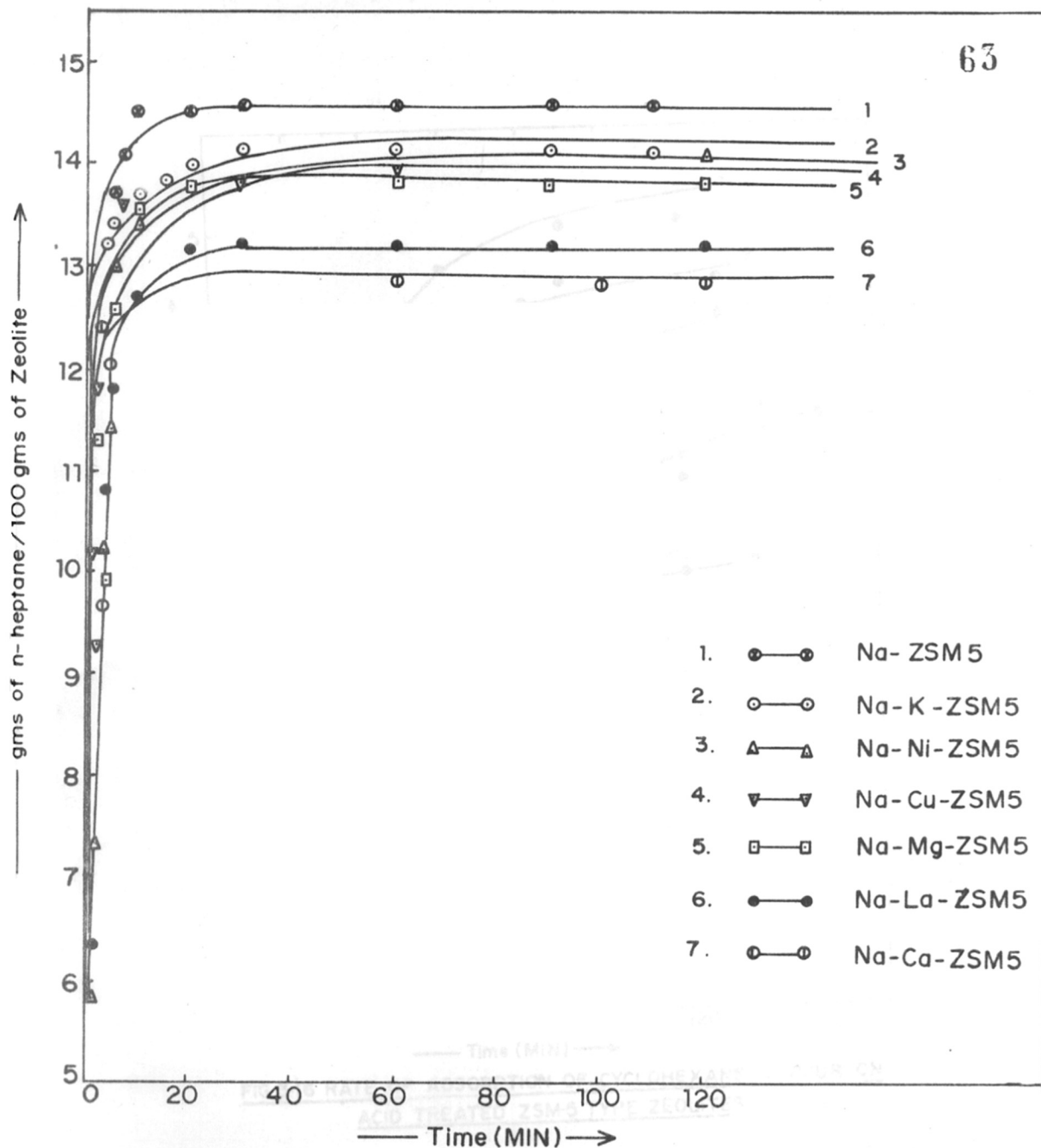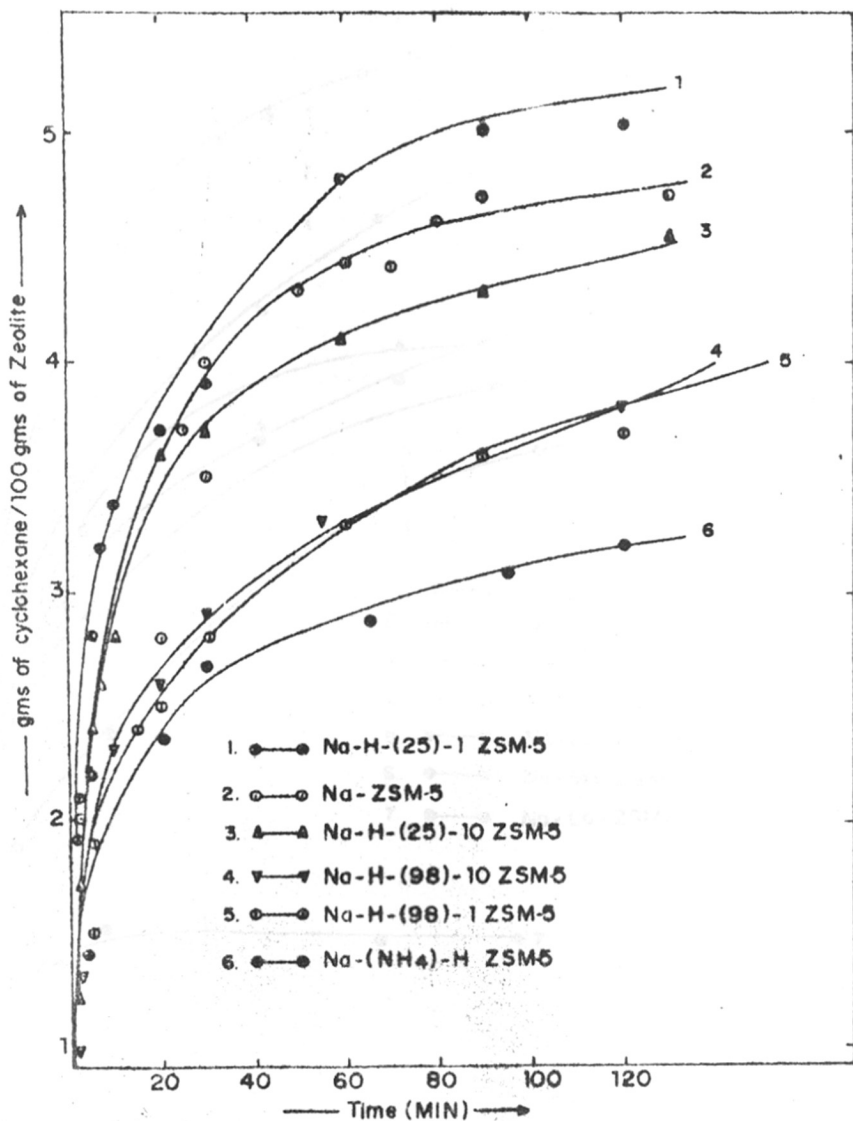
FIG. 3·14 RATE OF ADSORPTION OF n-HEPTANE VAPOUR ON ACID TREATED ZSM-5 TYPE ZEOLITES

FIG.3·15 RATE OF ADSORPTION OF n-HEPTANE VAPOUR ON CATION EXCHANGED ZSM5 TYPE ZEOLITES

FIG.3.16 RATE OF ADSORPTION OF CYCLOHEXANE VAPOUR ON ACID TREATED ZSM-5 TYPE ZEOLITES

Legend within figure:

1. ● Na-H-(25)-1 ZSM-5
2. ◐ Na-ZSM-5
3. ▲ Na-H-(25)-10 ZSM-5
4. ▼ Na-H-(98)-10 ZSM-5
5. ◉ Na-H-(98)-1 ZSM-5
6. ● Na-(NH₄)-H ZSM-5

Y-axis: gms of cyclohexane/100 gms of Zeolite
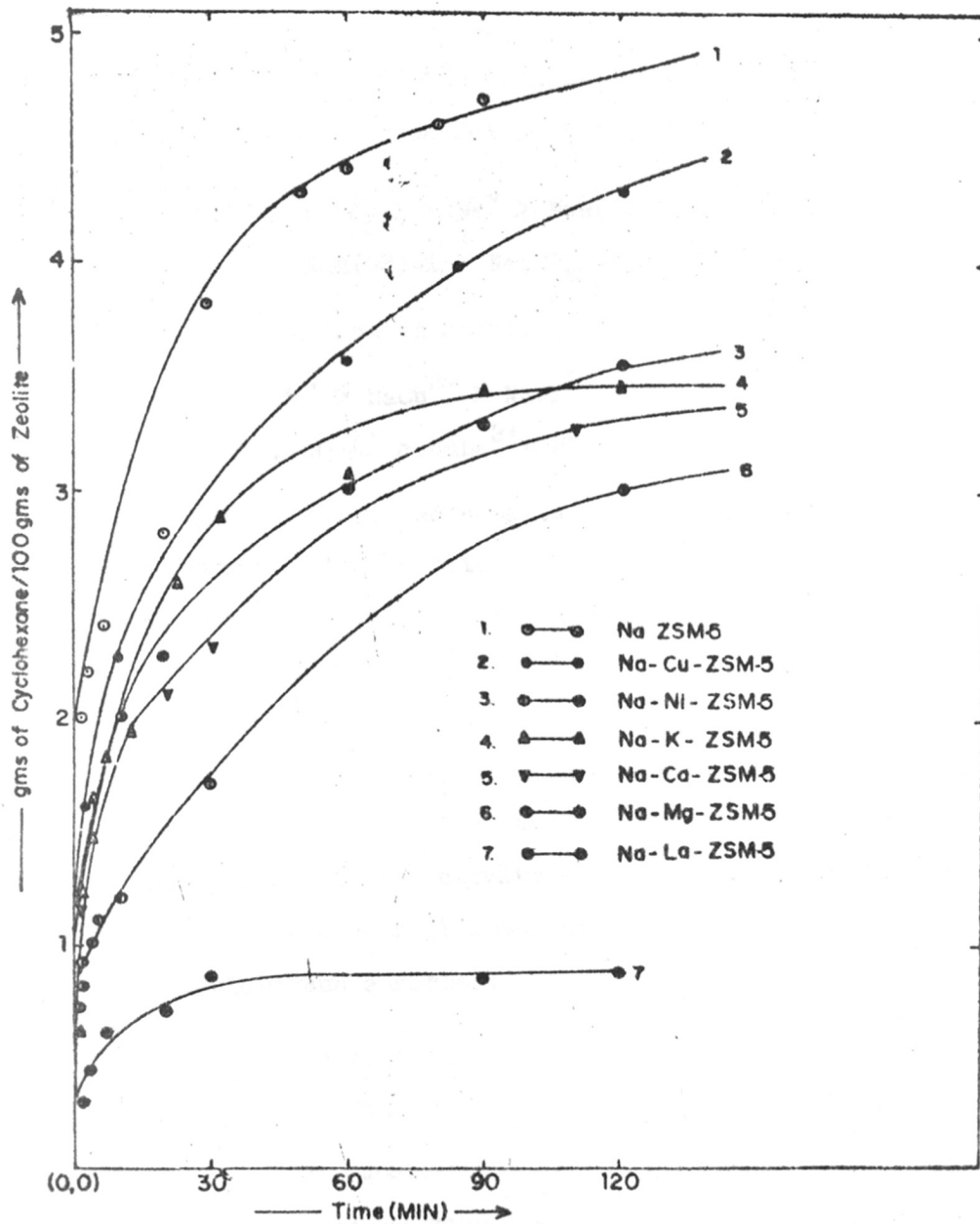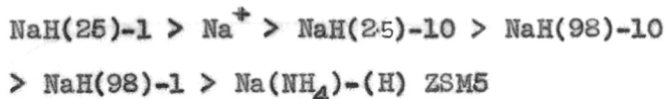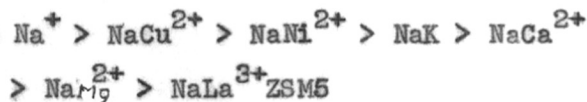X-axis: Time (MIN)

FIG.3·17 RATE OF ADSORPTION OF CYCLOHEXANE VAPOUR ON CATION EXCHANGED ZSM-5 TYPE ZEOLITES

attained even after 120 minutes exposure, the sorption
values at 120 minutes follow the sequence

$$NaH(25)-1 > Na^+ > NaH(25)-10 > NaH(98)-10$$
$$> NaH(98)-1 > Na(NH_4)-(H) \; ZSM5$$

for the acid treated samples, and

$$Na^+ > NaCu^{2+} > NaNi^{2+} > NaK > NaCa^{2+}$$
$$> NaMg^{2+} > NaLa^{3+} ZSM5$$

for the ion exchanged samples respectively. The remarkable
reduction in the sorption of cyclohexane in NaLaZSM5 may be
attributed to partial pore blocking (at the intersection)
of the zeolite. It is possible that while adsorption of
n-hexane occurs in both the pores and channel intersections,
cyclohexane having larger cross-sectional area is adsorbed
preferentially at pore intersections only. It has been found
that the catalytic activity for the xylene isomerization which
occurs at the channel intersections correlates with the amount
of cyclohexane adsorbed.

(D) ADSORPTION OF ORTHO,
META AND P-XYLENES

The uptake time curves for ortho, meta and para-
xylenes on various ZSM5 samples are illustrated in Figs. 3.18,
3.19 and 3.20 respectively. While like n-heptane, para-
xylene uptake is faster, the other two isomers are sorbed at
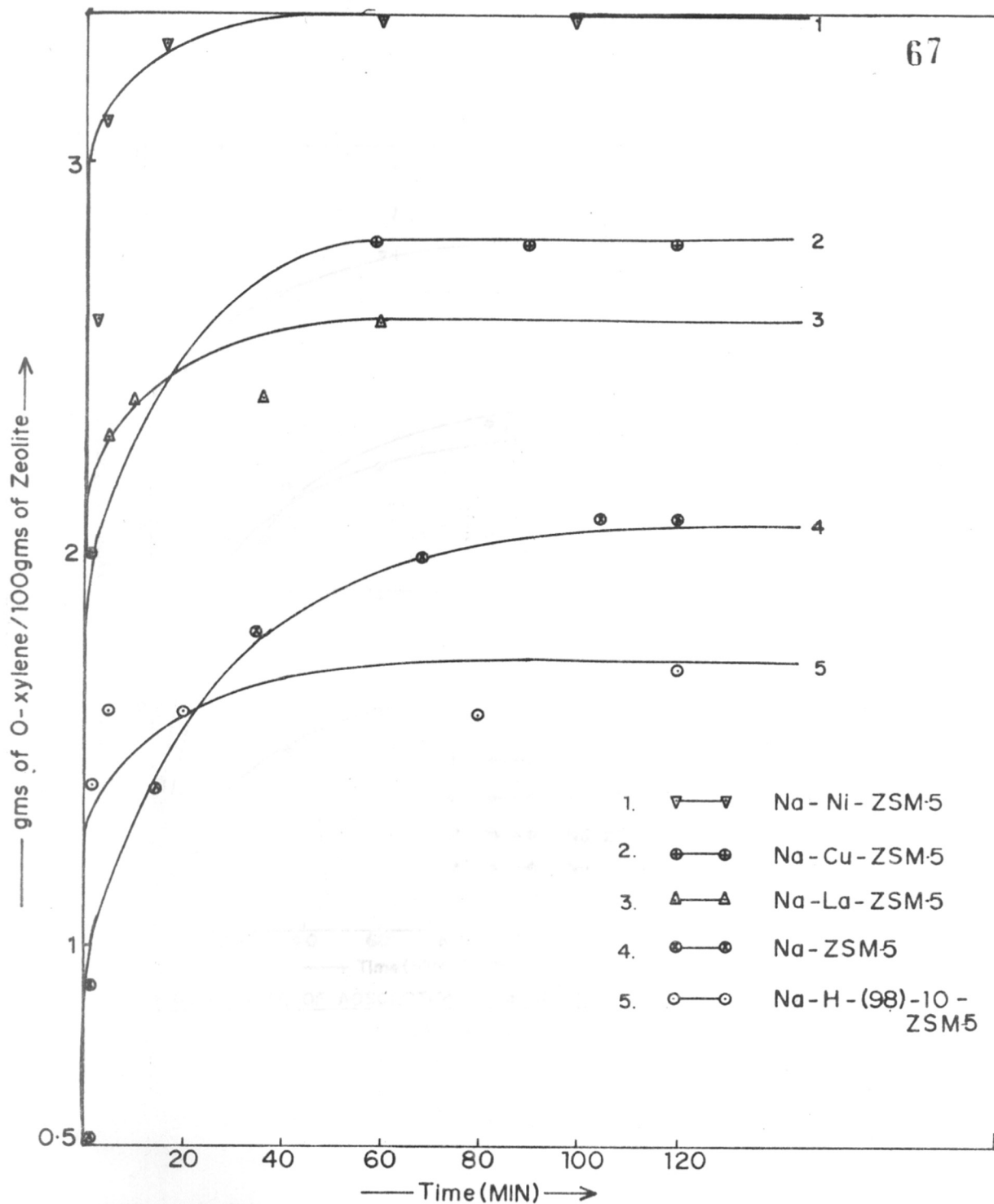a slower rate. The equilibrium sorption of the three isomers

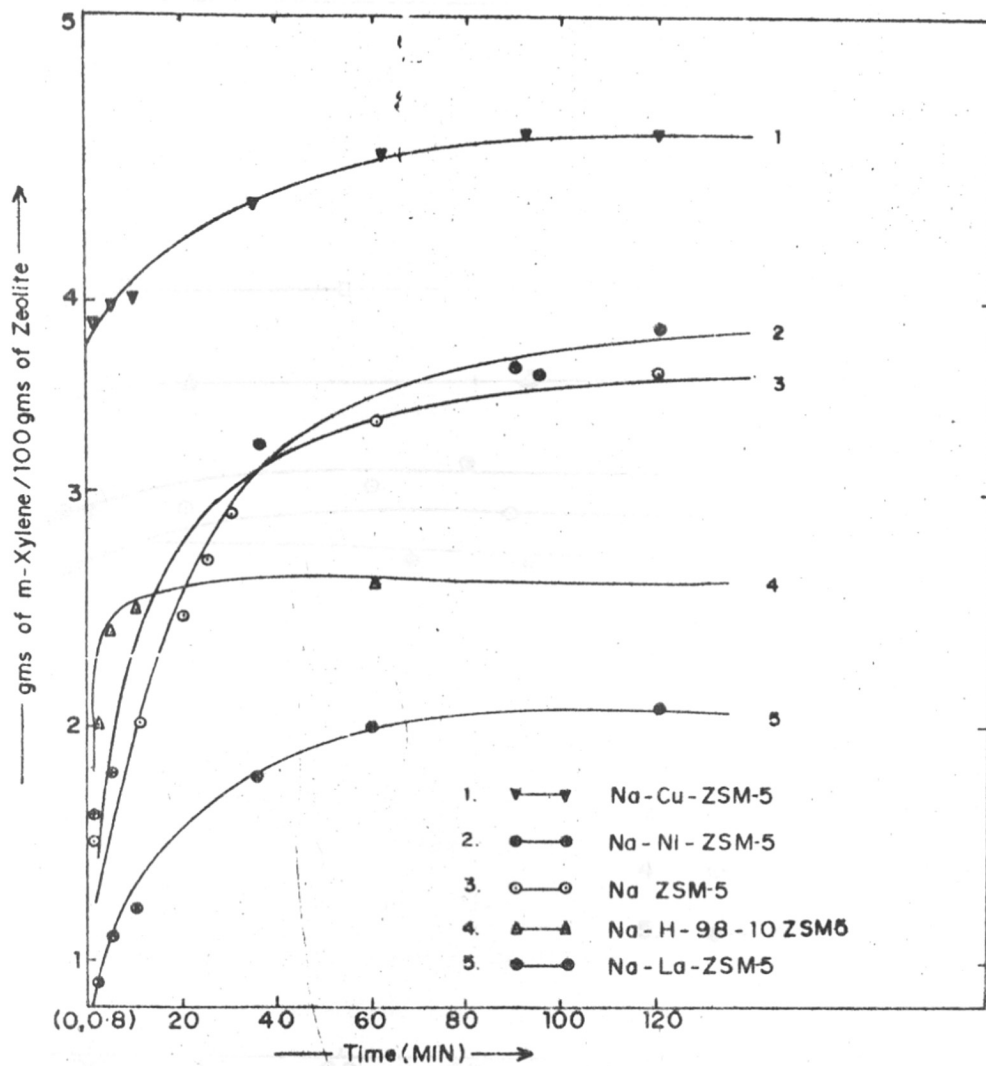FIG.3·18 RATE OF ADSORPTION OF O-XYLENE VAPOUR ON ZSM-5 TYPE ZEOLITES

FIG.3.19 RATE OF ADSORPTION OF m-XYLENE VAPOUR ON ZSM-5 TYPE ZEOLITES
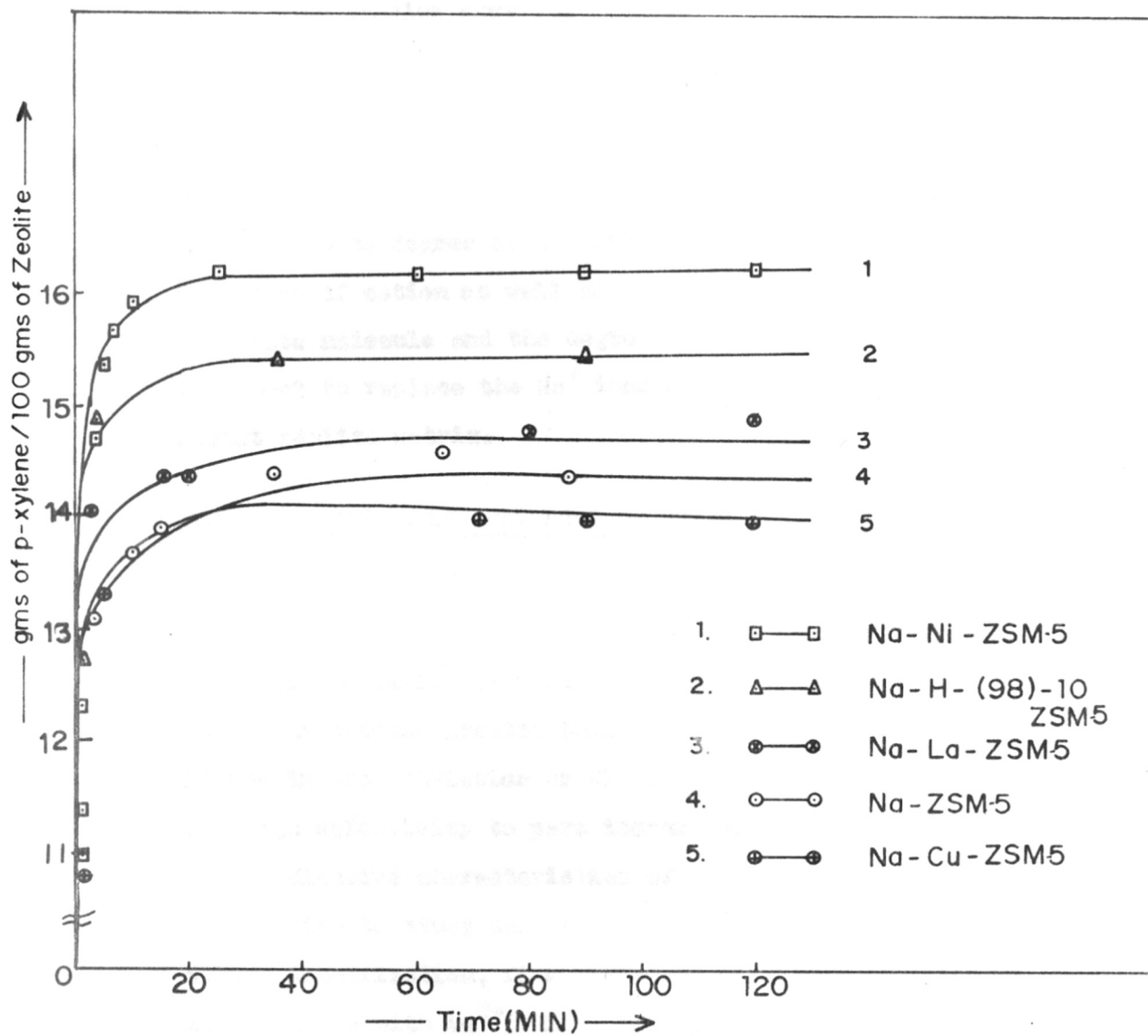
FIG.3·20 RATE OF ADSORPTION OF P-XYLENE VAPOUR ON ZSM·5 TYPE ZEOLITES

on the ZSM5 samples show the sequence

P-Xylene > Meta > Ortho.

The equilibrium uptake values for the various samples (in 120 minutes) are given in Table 3.8. The sorption data shows that the degree of adsorption is influenced strongly by nature of cation as well as the size and polarity of the adsorbate molecule and the degree of ion exchange or acid treatment to replace the Na^+ ions originally present in the parent zeolite matrix.

3.7   CATALYTIC REACTIONS OF ORTHO XYLENE ON ZSM5 ZEOLITES

It has been reported[61] that ZSM-type catalyst chemically modified by incorporation of phosphorus or magnesium possess greater than 95% selectivity to para xylene in the alkylation or disproportionation reactions. The high selectivity to para isomer was attributed[44] to the shape selective characteristics of the pores of ZSM5 zeolite. With a view to study the influence of exchanged cations on xylene isomerization, five ZSM5-type catalysts modified by ion exchange with La^{3+}, Ni^{2+}, Cu^{2+} H^+ (HZSM5) have been tested for ortho xylene isomerization reactions.

The reaction was carried out at 623 K in view of several earlier studies[62], which had established this temperature to be ideal. It was observed that at higher

TABLE - 3.8

WATER AND HYDROCARBON SORPTION

IN ZSM5 ZEOLITES

Catalyst	No. of molecules of adsorbate/unit cell					
	Water	N-Heptane	Cyclohexane	O-X	M-X	P-X
NaZSM5 (original)	41.3	8.23	3.27	1.33	2.01	8.41
Na-K-ZSM5	41.5	8.26	2.41	-	-	-
Na-Ni-ZSM5	43.7	8.54	2.52	1.98	2.16	8.95
Na-Cu-ZSM5	35.8	8.12	2.95	1.54	2.59	7.73
Na-Na-ZSM5	41.3	8.54	2.65	-	-	-
Na-Mg-ZSM5	38.7	8.1	2.7	2.58	2.55	8.04
Na-H-(25)-1 ZSM-5	40.4	8.25	3.25	-	-	-
Na-25-10 ZSM-5	38.00	8.31	3.36	-	-	-
Na-H-(98)-1 ZSM-5	39.9	8.06	2.65	-	-	-
Na-H-(98) -10 ZSM-5	41.4	8.10	2.58	0.932	1.43	8.51
Na-La-ZSM5	33.98	7.69	0.59	1.49	1.18	8.16
Na-Ca-ZSM5	39.13	7.53	2.19	-	-	-
Na-NH$_4$- (H)-ZSM5	36.00	7.91	2.20	-	-	-

Anderson et al J. Cat. Vol. 58, 114-130 (1979)
P-xylene = 5.56 molecules/unit cell at 293^{0}K
and in 10 minutes.

temperatures dealkylation of xylene to toluene and methane
and disproportionation to C_9 aromatics and toluene takes place.
At lower temperatures conversion of ortho xylene is too low.
The activity for isomerization reaction is expressed in terms
of PATE (p-xylene approach to equilibrium) and is calculated
using the following expression:

$$PATE = \frac{\% \text{ P-xylene in product among the isomers} - \% \text{ Para-xylene in the feed among the isomers}}{\% \text{ P-xylene at equilibrium} - \% \text{ P-xylene in the feed.}}$$

The reaction products were collected every hour and analysed
by G.C. (Chapter II). The product distribution obtained using
five typical ZSM5 samples is illustrated in Table 3.9. It was
observed that all catalyst samples except NaCuZSM5 showed
stable activity during the period of experiment. Deactivation
with time which is a characteristic of all catalysed reactions
is observed at very large time on stream with ZSM type catalyst.

The experimental data presented in Table 3.9 indicates
that out of the five catalyst samples tested for the ortho
xylene conversion reaction only HZSM5 is a suitable catalyst. The
ion exchanged ZSM5 catalyst showed low ortho xylene conversions
and hence are not suitable for commercial exploitations and
any commercial catalyst suitable for the reaction would be one
based upon HZSM5 zeolite which has been suitably modified to
improve life and PATE.

TABLE - 3.9

CATALYTIC CONVERSION OF ORTHO XYLENE ON ZSM5

ZEOLITES - PRODUCT DISTRIBUTION

Catalyst	B	T	P-Xyl	M-Xyl	O-Xyl	C_9^+	α^*	PATE
1. Na2SM5	0.660	6.766	16.264	38.452	34.746	3.941	65.2	73
2. NaLa2SM5	0.435	3.289	12.908	20.174	62.282	0.749	38.0	57
3. NaNi2SM5	0.403	3.668	14.427	34.405	45.080	1.948	54.92	54.22
4. NaCu2SM5	0.494	3.856	15.743	29.117	48.749	1.874	51.30	70.91
5. Na-H-(98)-10	0.714	10.130	16.451	42.475	22.577	7.47	77.423	86.09

B = Benzene, T = Toluene, P-Xyl, M-Xyl, O-Xyl = para, meta, ortho xylene respectively.

α^* = % ortho xylene conversion.

The catalyst presently tested i.e. NaH(98)-10 gave an ortho xylene conversion of 70% and PATE of 85%. This activity was stable beyond the 12 hours tested in a separate[62,63] study. The increase in C_9 is in the line with the greater activity of the catalyst.

SUMMARY

The ZSM5 type zeolite is a new shape selective zeolite belonging to a pentasil family of crystalline alumino silicates and has been extensively studied as a commercial catalyst for isomerization, alkylation, disproportionation, dewaxing and selectoforming.

The ZSM5 type zeolite has been prepared using indigeneous raw materials and characterized by X-ray diffraction, infrared spectroscopy, scanning electron microscopy, chemical analysis, thermal analysis (DTA, TG, DTG), adsorption of argon, water and organic vapours and catalytic reaction for the conversion of ortho xylene.

A series of acid treated and ion exchanged forms, NaHZSM5 and NaM^{n+}ZSM5 where M^{n+} represents K$^+$, Cu^{2+}, Ni^{2+}, Ca^{2+}, Mg^{2+} and La^{3+} have been prepared. The structural and catalytic properties of the modified ZSM5 zeolites have been examined by employing the above physico-chemical techniques.

The X-ray powder diffraction patterns of the acid treated and cation exchanged samples did not show significant changes in the d values (interplaner spacings) or intensities of the diffraction lines. Further, the results indicate a high stability of ZSM5 structure to acid treatment (1N HCl), which can be an alternate route for the preparation of H form of ZSM5 in the form of an active catalyst for hydrocarbon conversion reactions.

The scanning electron microscopy revealed distinct differences in the amorphous and crystalline phases during the course of crystallisation. The IR spectra revealed that ZSM5 structure possesses a characteristic absorption band at 550 cm^{-1}, which has been assigned to highly distorted double 5 membered ring in the pentasil structure.

The thermograms indicated two step weight loss, the first step due to dehydration and the second due to the decomposition of the occluded organic material in the pores of the ZSM5 structure. Further, the DTA thermograms showed an endotherm due to desorption of water from the zeolite cavities and three well resolved exotherms which have been assigned to the decomposition of the occluded material. No structural changes in the ZSM5 framework were observed upto 1275 K indicating high thermal stability of the zeolite. This was true for all the ion exchanged and acid treated ZSM5 zeolite samples.

The adsorption of argon at $77^{o}K$ was fast and attained equilibrium values at relatively low pressures. From the argon adsorption at $77^{o}K$, the surface area and pore volume of a few ZSM5 samples have been estimated. The applicability of Dubinin equation for the calculations of free energy of adsorption (ΔG^{o}) has been tested. The sorption capacity was maximum in acid treated sample and minimum in La^{3+} exchanged zeolite. The latter has attributed to a partial blocking in the ZSM5 channel intersection.

The water adsorption rate and equilibrium capacity decreased with exchange of Na with multivalent cations as also with acid treatment of the zeolite. The modified zeolites readily sorbed n-heptane while the uptake of cyclohexane which has larger molecular size than pore dimensions was slow and equilibrium did not reach even after 120 minutes exposure of the zeolite to the cyclohexane vapour.

The kinetics of sorption of ortho, meta and para xylenes on the ZSM5 type zeolites revealed that the uptake of para isomer was fastest and equilibrium reached within 5 to 20 minutes exposure. Relatively, the meta isomer was sorbed at a slower rate. The equilibrium sorption values followed the sequence

para >> ortho > meta.

The critical dimensions of ortho, meta xylenes and cyclohexane are larger than para xylene and therefore their uptake is slow and smaller as compared to the para isomer. Moreover, the critical dimension of ortho xylene (6.8Å) is slightly larger than the pore dimensions of the ZSM5 channel. As a result, the uptake is slow and small.

The activity of modified ZSM5 samples for the conversion of ortho xylene was evaluated at 623 K. The reaction products were analysed by G.C. and the % conversion of ortho xylene and PATE for p-isomer for the 5 catalyst samples has been estimated. Further, the stability of the

catalyst under optimum conditions of reaction was determined. The HZSM5 based catalyst showed optimum conversion and stable catalytic life over a period of 12 hours.

From the present studies it may be concluded that the sorption and catalytic properties of ZSM5 zeolites depend upon the nature of cation present. The H form of the ZSM5 zeolite showed optimum conversion of ortho xylene and stable catalytic activity.

REFERENCES

1. B. Cronstedt, Akad. Handl. Stockholm, 18, 120 (1756).

2. A. Damour, Ann. Mines, 17, 191 (1840).

3. F. Grandjean, Compt. rendn, 149, 866 (1909).

4. R. M. Barrer, J. Chem. Soc. Ind. Ed., 64, 133 (1945).

5. R. M. Barrer and D. A. Ibbitson, Trans. Far. Soc., 40, 195 (1944).

6. R. M. Milton, cf "Molecular Sieve" Soc. Chem. Ind. London, 1968, p. 199.

7. D. W. Break in "The Properties and Applications of Zeolites (R. P. Townsend ed.), 33, 391 (1980).

8. R. M. Barrer and P. J. Denny, J. Chem. Soc, p. 971 (1961).

9. G. T. Kerr, J. Inorg. Chem., 5, 1537 (1966).

10. R. Aiello and R. M. Barrer, J. Chem. Soc. A p. 1470 (1970).

11. C. J. Plank, E. J. Rosinski and M. K. Rubin, Brit. Patent 1,297,256 (1972).

12. R. J. Argeuer and G. R. Landolt, U.S. Patent, 3,702,886 (1972).

13. V. Leclwze and L. B. Sand, 5th International Conference Zeolites, Naples (1980).

14. N. Y. Chen and W. E. Garwood, J. Catal., 52, 453 (1978).

15. E. G. Derouane and J. C. Vedrine, J. Mol. Catal., 8, 479 (1980).

16. S. L. Meisel, J. P. McCullough, P. B. Weisz, Chem. Tech. 86 (1976).

17. G. T. Kokotailo, S. L. Lawton, D. H. Olson and W. M. Meier, Nature, 272, 437 (1978).

18. E. L. Wu, S. L. Lawton, D. H. Olson, A.C. Rohrman, Jr. and G.T. Kokotailo, J. Phys. Chem., 83 (21), 2777 (1979).

19. E. M. Flanigen, J. M. Bennett, R.W. Grose; J. P. Cohen, R. L. Patton, R. M. Kirchner and J. V. Smith, Nature, 271 512 (1978).

20. J. R. Anderson, K. Foger, T. Mole, R.A. Rajadhyaksha and J. V. Sanders, J. Catal. 58, 44 (1979).

21. D. H. Olson, W. O. Haag and R. M. Lago, J. Catal, 61, 370 (1980).

22. P. Chu and F.G. Dwyer in Intra Zeolite Chemistry – ACS Symposium Series 218, Amer. Chem.Soc. (1983), p.59.

23. A. Gulfaz and L. B. Sand, Adv. Chem. Ser., 121, 140 (1973).

24. S.B. Kulkarni, V.P. Shiralkar, A. N. Kotasthane, R.B. Borade and P. Ratnasamy, Zeolites, 2, 313 (1982).

25. E. Dempsey, G.H. Kuhl and D. H. Olson, J. Phys. Chem., 73, 387 (1969).

26. E. M. Flanigen, H. Khatami and H. A. Szymanki, Adv. Chem. Ser. 102, 374 (1973).

27. H. Topsøe, K. Pederson and E.G. Derouane, J. Catal., 70, 41 (1981).

28. D. W. Breck 'Zeolite Molecular Sieves', John Wiley and Sons, New York (1974).

29. J. A. Verdel, Oil Gas Jour., 67, 63 (1969).

30. H. Anon, Hydrocarbon Process, 48, 155 (1969).

31. R. Allen, L. Yats, J. Amer. Chem. Soc., 81, 5289 (1959).

32. J. D. Kemp, V. U.S. Patent, 2527824 (1950).

33. K. L. Hanson, A. J. Engel, A.I.Ch.E.J., 2, 260 (1967).

34. D. Marsicobetre, N.S. Gnep, M. Guisnet, Rev. Port, Quim, 18, 313 (1976).

35. W.W. Kaeding, C., Chu, L. B. Young, B. Weinstein., S. A. Butter, J. Catal., 67, 159 (1981).

36. A. G. Vedenjaeva Vypkhim, 2, 212 (1971).

37. J. W. Ward, J. Catal., 13, 321 (1969).

38. H. Klume et al., German Patent, 42641 (1975).

39. D. H. Olson and W. O. Haag, U.S. Patent 4169282 (1979).

40. P.B. Weisz, Pure & Appl. Chem 52, 2091 (1980)

41. R. M. Barrer and E. A. D. White, J. Chem. Soc. 156 (1961).

42. A. I. Regis, L. B. Sand, C. Calmon and M.E. Gilwood, J. Phys. Chem., 64, 1567 (1980).

43. F. E. Schwochow and G. W. Heinz, Adv. Chem. Ser., 101, 102 (1971).

44. R. J. Argauer, G. R. Landolt, U.S. Pat. 3,702,886 (1972).

45. F. G. Dwyer, E. E. Jenkins, U.S. Pat., 3,941,871.

46. R. W. Grose and E. M.Flanigen, U.S. Pat., 4,257,885.

47. N. Y. Chen., J. N. Miale and N. Y. Reagen, U.S. Pat., 4,112,056.

48. S. B. Kulkarni, V.P. Shiralkar, A. N. Kotasthane, R.B. Borade and P. Ratnasamy, Zeolites, 2, 313 (1982).

49. K. J. Chao, T.C. Tasi, M.S. Chen and I. Wang, J. Chem. Soc., Far. Trans. I 77, 547 (1981).

50. P. A. Jacobs, E.G. Derouane and P. Weitkamp., J. Chem. Soc., Chem. Comm. 591 (1981).

51. F. Paulik, J. Paulik and L. Erdey, Talanta, 12, 1405 (1976).

52. P. A. Jacobs, H. K. Bayer and J. Valyon, Zeolites, 1, 161 (1981).

52A A. Erdem and L. B. Sand, J. Catal., 60, 241 (1979).

53. G. Conduries, C. Naccache and J.C. Vedrine, J. Chem. Soc. Chem. Comm. 1413 (1983).

54. R.B. Borade, Ph.D. Thesis, University of Poona (1983).

55. M.R.S. Manton and J.C. Davidtz, J. Catal, 60, 156 (1979).

56. E. M. Flanigen in "Proc. 5th Internatl. Conf. Zeolites" Ed. L.V.C. Rees, Naples, Heyden and Sons, London, 760 (1980).

57. R. Mostowiez and L.B. Sand, Zeolites, 2, 143 (1982).

58. G. V. Tsitrishvili and T. G. Andronikastivili, Adv. Chem. Ser., 102, 271 (1971).

59.   M.F. L. Johnson, J. Catal, 52, 425 (1978).

60.   G.V. Tritristivili, Adv. Chem. Ser., 121, 291 (1973).

61.   N. Y. Chen, W.W. Kaeding, and F. G. Dwyer, J. Am. Chem. Soc., 101, 6783 (1979).

62.   I. Balkrishnan, B.S. Rao, C.V. Kavedia, G.P. Babu, S.B. Kulkarni and P.Ratnasamy, Chem. Ind., 410, June 19 (1982).

63.   G. P. Babu, Ph.D. Thesis (1983), Poona University.